Article

Rhizobia–diatom symbiosis fixes missing nitrogen in the ocean

https://doi.org/10.1038/s41586-024-07495-w

Received: 16 November 2023

Accepted: 30 April 2024

Published online: 9 May 2024

Open access

Check for updates

Bernhard Tschitschko[1,6], Mertcan Esti[1], Miriam Philippi[1,7], Abiel T. Kidane[1], Sten Littmann[1], Katharina Kitzinger[1,2], Daan R. Speth[1,8], Shengjie Li[1], Alexandra Kraberg[3], Daniela Tienken[1], Hannah K. Marchant[1,4], Boran Kartal[1,5], Jana Milucka[1], Wiebke Mohr[1] & Marcel M. M. Kuypers[1]✉

Nitrogen (N_2) fixation in oligotrophic surface waters is the main source of new nitrogen to the ocean[1] and has a key role in fuelling the biological carbon pump[2]. Oceanic N_2 fixation has been attributed almost exclusively to cyanobacteria, even though genes encoding nitrogenase, the enzyme that fixes N_2 into ammonia, are widespread among marine bacteria and archaea[3–5]. Little is known about these non-cyanobacterial N_2 fixers, and direct proof that they can fix nitrogen in the ocean has so far been lacking. Here we report the discovery of a non-cyanobacterial N_2-fixing symbiont, '*Candidatus* Tectiglobus diatomicola', which provides its diatom host with fixed nitrogen in return for photosynthetic carbon. The N_2-fixing symbiont belongs to the order Rhizobiales and its association with a unicellular diatom expands the known hosts for this order beyond the well-known N_2-fixing rhizobia–legume symbioses on land[6]. Our results show that the rhizobia–diatom symbioses can contribute as much fixed nitrogen as can cyanobacterial N_2 fixers in the tropical North Atlantic, and that they might be responsible for N_2 fixation in the vast regions of the ocean in which cyanobacteria are too rare to account for the measured rates.

Nitrogen is an essential component of all living organisms and limits life in the ocean. Atmospheric N_2 gas is the largest reservoir of freely accessible nitrogen, but it is biologically available only to microorganisms that carry the nitrogenase metalloenzyme and thus can fix N_2 into ammonia[7]. Even though a wide diversity of marine bacteria and archaea encode nitrogenase, the bulk of nitrogen fixation in the ocean has been attributed to cyanobacteria (ref. 4 and references therein). These phototrophs are capable of both free-living and symbiotic lifestyles, and can directly or indirectly contribute to carbon fixation and export production in the regions where they are abundant, such as oligotrophic coastal waters and margins of subtropical gyres[8]. Notably, in vast regions of the ocean, such as the centres of subtropical gyres, cyanobacterial N_2 fixers are too rare to account for the measured rates of N_2 fixation. Instead, a role of non-cyanobacterial N_2 fixers has been invoked, on the basis of the abundance of nitrogenase-encoding gene sequences (*nifH*), most of which belong to uncultured proteobacteria (for example, refs. 3,5,9–11). So far, the most frequently detected non-cyanobacterial N_2 fixer is the so-called gamma-A, named after its *nifH* gene phylogeny that clusters within the Gammaproteobacteria[12]. This enigmatic microorganism has been shown to be distributed in most world oceans, and its potential activity has been inferred from in situ *nifH* transcription[13,14]. To date, however, there is no proof that gamma-A fixes N_2 in situ, and essentially all aspects of its physiology remain unknown.

An N_2-fixing rhizobial diatom endophyte

We investigated the role of non-cyanobacterial N_2 fixation in the tropical North Atlantic during an expedition in January–February 2020. This region is responsible for around 20% of oceanic N_2 fixation[8], and cyanobacteria can only explain approximately half of the rates measured in the region[10]. We detected high N_2 fixation rates of up to 40 nmol N l^{-1} d^{-1} in the surface waters (Extended Data Table 1), and the presence of both cyanobacterial and heterotrophic N_2 fixers—specifically, gamma-A—was confirmed by metagenomic sequencing (Extended Data Fig. 1a). Gamma-A *nifH* sequences were retrieved only from the large size fraction (greater than 3 µm) suggesting particle attachment or an association with a host organism (Extended Data Fig. 1a). We recovered a near-complete metagenome-assembled genome (MAG; 1.7 Mb, 37.8% GC, 98% completion with 0% redundancy) containing the gamma-A *nifH* gene, as well as a complete cluster of rRNA genes (Supplementary Table 1). Although the retrieved *nifH* sequence clustered within the Gammaproteobacteria as previously reported[3,14,15] (Extended Data Fig. 2), both 16S-rRNA-gene-based and whole-genome-based taxonomy[16] firmly placed this MAG within the alphaproteobacterial family *Hyphomicrobiaceae* (Fig. 1a). This family belongs to the order Rhizobiales, which comprises the prominent rhizobial symbionts of nodule-forming terrestrial legumes[6,17,18]. In addition to *nifH*, most other genes of the *nif* regulon are of gammaproteobacterial origin, including

[1]Max Planck Institute for Marine Microbiology, Bremen, Germany. [2]Centre for Microbiology and Environmental Systems Science, Division of Microbial Ecology, University of Vienna, Vienna, Austria. [3]Alfred Wegener Institute, Helmholtz Centre for Polar and Marine Research, Bremerhaven, Germany. [4]MARUM – Centre for Marine Environmental Sciences, University of Bremen, Bremen, Germany. [5]School of Science, Constructor University, Bremen, Germany. [6]Present address: Department of Microbiology, University of Innsbruck, Innsbruck, Austria. [7]Present address: Alfred Wegener Institute, Helmholtz Centre for Polar and Marine Research, Bremerhaven, Germany. [8]Present address: Centre for Microbiology and Environmental Systems Science, Division of Microbial Ecology, University of Vienna, Vienna, Austria. ✉e-mail: mkuypers@mpi-bremen.de

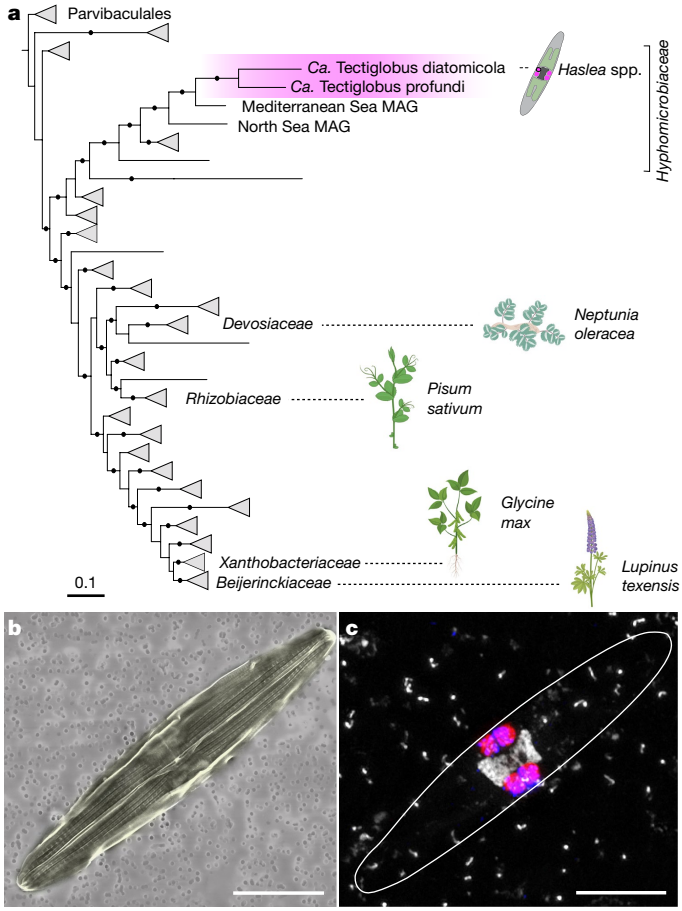

Fig. 1 | Phylogeny and visualization of *Candidatus* Tectiglobus diatomicola and its diatom host. a, Maximum likelihood phylogenetic tree of concatenated bacterial marker genes from the order Rhizobiales, showing the placement of *Ca*. T. diatomicola within the *Hyphomicrobiaceae* family (see Methods). The novel genus *Ca*. Tectiglobus, comprising *Ca*. T. diatomicola and its closest relative *Ca*. T. profundi, is highlighted in pink. Families within the Rhizobiales that contain known N_2-fixing legume symbionts and their exemplary host plants are shown. The order Parvibaculales was used as an outgroup. Black dots indicate more than 95% bootstrap support. Scale bar indicates amino acid substitutions per site. Plant icons were designed by Freepik (*Neptunia oleracea*) or created with BioRender.com. **b**,**c**, False coloured scanning electron microscopy (SEM) image (**b**) and confocal laser scanning microscopy image (**c**) of a *Haslea* diatom. Four *Ca*. T. diatomicola cells (pink, overlay of Hypho1147 and Hypho734 fluorescence in situ hybridization (FISH) probes; Extended Data Table 2) were detected next to the host nucleus (white; stained with DAPI). Scale bars, 5 µm.

nifD and *nifK*, which encode the catalytic component of the nitrogenase; *nifE*, *nifN* and *nifB*, which encode the iron-molybdenum cofactor assembly proteins; and *nifS*, which is involved in metallocluster biosynthesis (Extended Data Fig. 2a). Almost all other genes in the gamma-A MAG are of alphaproteobacterial origin (Supplementary Table 1). On the basis of these results, we conclude that the gamma-A N_2 fixer is, in fact, an alphaproteobacterium that has acquired its nitrogenase genes through horizontal gene transfer from a gammaproteobacterial donor. Besides gamma-A, several other bacteria, including members of the order Rhizobiales, obtained their nitrogenase genes through horizontal gene transfer from a gammaproteobacterial donor (Extended Data Fig. 2b). Such horizontal gene transfer across classes, resulting in the acquisition of nitrogenase genes, has been reported previously for other N_2 fixers[19,20].

We name the newly discovered species '*Candidatus* Tectiglobus diatomicola' within a novel genus '*Candidatus* Tectiglobus' (see Methods for etymology). One other marine MAG from the North Pacific, which we now name '*Candidatus* Tectiglobus profundi', is affiliated with this novel genus, with 72% average amino acid identity with *Ca*. T. diatomicola (Supplementary Methods). Compared with their closest relative, a MAG from the Mediterranean Sea, both *Ca*. Tectiglobus species have a substantially reduced genome size (around 1.7 Mb versus around 5 Mb) and a strongly decreased GC content (around 38% versus around 54%) (Extended Data Fig. 3), which are features typical of endosymbionts[21]. Notably, a similar reduction in genome size and GC content is observed for the N_2-fixing cyanobacterial endosymbiont *Candidatus* Atelocyanobacterium thalassa, or UCYN-A, which lives in symbiosis with a haptophyte alga[22,23]. Thus, the genome properties of *Ca*. T. diatomicola, together with its presence in the large size fraction, strongly indicate a host-associated lifestyle.

We designed specific 16S rRNA oligonucleotide probes to visualize *Ca*. T. diatomicola (Extended Data Table 2), and found hybridized cells (1–2 µm cocci) that were located exclusively inside diatom hosts (Fig. 1b,c and Extended Data Fig. 4). The hosts showed large variation in cell sizes (20–58 µm long and 3–8 µm wide), probably representing different diatom life stages[24]. Typically, four *Ca*. T. diatomicola symbionts were observed in the proximity of the centrally located host nucleus, with some dividing hosts containing up to eight symbionts (Fig. 1c and Extended Data Fig. 4). On the basis of scanning electron micrographs combined with fluorescence microscopy, the host was identified as a pennate diatom likely to belong to the genus *Haslea* within the *Naviculaceae* family (Extended Data Fig. 4; see also Supplementary Information). Indeed, sequences belonging to this genus were recovered from the metagenome with the highest abundance of *Ca*. T. diatomicola (Supplementary Table 2, see also Methods). *Haslea* are ubiquitous marine diatoms that are found in surface waters (Extended Data Fig. 5a) and coastal sediments throughout the world's oceans[25], but they have not previously been reported to contain N_2-fixing symbionts. Most marine diatom species that form associations with N_2-fixing cyanobacteria are centric diatoms such as *Hemiaulus*, *Rhizosolenia* and *Chaetoceros*[26]. The new *Haslea* hosts thus expand the range of diatoms that can associate with N_2-fixing symbionts. More importantly, all so-far-known N_2-fixing symbionts of diatoms belong exclusively to the cyanobacteria[27,28]. Our discovery represents the first example—to our knowledge—of a symbiosis between a diatom and a non-cyanobacterial N_2-fixing microorganism.

Host–symbiont metabolic interactions

To gain insights into the metabolic interactions between *Ca*. T. diatomicola and its *Haslea* host, we studied the *Ca*. T. diatomicola genome together with its in situ transcriptome. The *Ca*. T. diatomicola genome encodes all genes necessary for N_2 fixation to ammonia, most of which were highly transcribed (Fig. 2a,b and Supplementary Table 1). These include key genes encoding the nitrogenase (*nifH*, *nifD* and *nifK*) and the iron-molybdenum cofactor assembly proteins (*nifE*, *nifN* and *nifB*).

Ca. T. diatomicola has a strongly reduced genome size, but the genome still encodes core carbon-processing pathways such as glycolysis and the tricarboxylic acid (TCA) cycle, which are present in many heterotrophic bacteria. However, on the basis of the low transcription of glycolysis genes (Supplementary Table 1), *Ca*. T. diatomicola probably does not grow on sugars. Instead, many genes involved in the TCA cycle were highly transcribed, in particular malate (*mdh*) and succinate (*sdh*) using enzymes (Fig. 2a,b and Supplementary Table 1), indicating growth on dicarboxylic acids. The dicarboxylates can be converted via pyruvate to acetyl-CoA, driving the TCA cycle independent of the glycolysis pathway (Fig. 2b). This is supported by the high transcription of genes encoding a TRAP-type dicarboxylic acid transporter (*dctP*, *dctQ* and *dctM*) and enzymes that decarboxylate malate (*maeB*) and oxaloacetate (*pckA* and *pyk*) to phosphoenolpyruvate and pyruvate. On the basis of the combined genomic and transcriptomic data, it seems that the N_2-fixing *Ca*. T. diatomicola provides ammonia to the *Haslea*

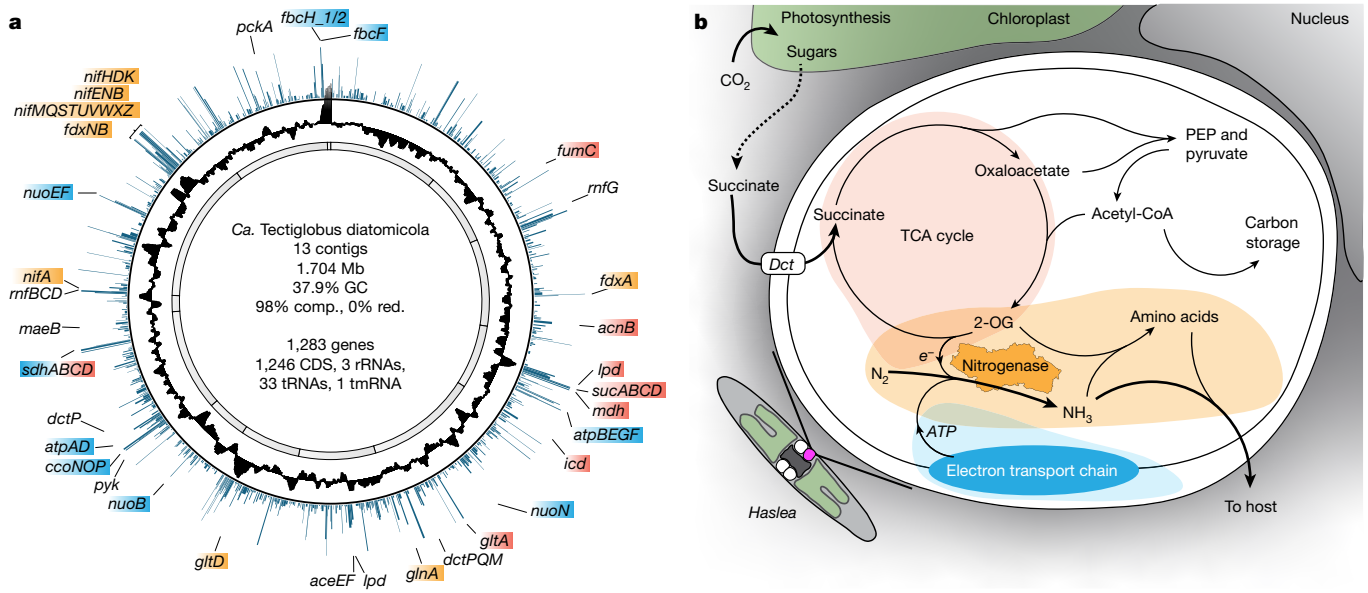

Fig. 2 | Genome properties, gene transcription and proposed metabolism of the *Candidatus* Tectiglobus diatomicola symbiont. a, Circular representation of the *Ca*. T. diatomicola genome with 13 encoding contigs (grey), GC content (black) and the average transcription of protein-coding genes as transcripts per million (TPM) (blue; TPM values higher than 800 were cut off). Genes related to N_2 fixation (orange), electron transport chain and ATP generation (blue) and the TCA cycle (red) are highlighted. CDS, coding sequence; comp., completeness; red., redundancy; tmRNA, transfer-messenger RNA. **b**, Schematic of the proposed metabolic potential of *Ca*. T. diatomicola (white) and its interactions with *Haslea* (grey and green), indicating the transfer of fixed nitrogen from the N_2-fixing symbiont in return for diatom-derived C_4-dicarboxylic acids, such as succinate. Proteins and corresponding gene names are: Complex I (NADH–quinone oxidoreductase, *nuoBNEF*), Complex II (succinate dehydrogenase, *sdhABCD*), Complex III (cytochrome *b*/*c*1, *fbcH_1/2*, *fbcF*), Complex IV (cbb_3-type oxidase, *ccoNOP*), Complex V (ATP synthase, *atpABDEGF*); fumarate hydratase (*fumC*); aconitate hydratase (*acnB*); 2-oxoglutarate dehydrogenase (*sucAB*, *lpd*); succinyl-CoA synthetase (*sucCD*); malate dehydrogenase (*mdh*); isocitrate dehydrogenase (*icd*); citrate synthase (*gltA*); nitrogenase (*nifHDK*) and its ancillary proteins (*nifAENBMQSTUVWXZ*) and ferredoxins (*fdxABN*); rnf complex (*rnfBCD*); dicarboxylic acid transporter (*dctPQM*); pyruvate dehydrogenase (*aceEF*, *lpd*); pyruvate kinase (*pyk*); malic enzyme (*maeB*); and phosphoenolpyruvate carboxykinase (*pckA*). 2-OG, 2-oxoglutarate; PEP, phosphoenolpyruvate.

diatom host in return for dicarboxylic acids (Fig. 2b). This metabolite exchange is strongly reminiscent of the metabolic interaction in rhizobia–legume symbioses[29,30], in which N_2-fixing rhizobia grow on host-provided dicarboxylic acids, such as succinate and malate, and in return provide fixed nitrogen to the host plant. By contrast, in symbioses between marine diatoms and N_2-fixing cyanobacteria, both partners are photosynthetic and grow on inorganic carbon[31].

Notably, *Ca*. T. diatomicola seems to have lost its low-affinity terminal oxidase (Supplementary Table 1), which is typically present in other members of the *Hyphomicrobiaceae* family, with the notable exception of *Ca*. T. profundi (Supplementary Table 3). Instead, *Ca*. T. diatomicola encodes and highly transcribes the high-affinity cytochrome cbb_3-type (*ccoN*, *ccoO* and *ccoP*) terminal oxidase (Fig. 2a, Extended Data Fig. 6 and Supplementary Table 1), which is used for respiration under low-oxygen conditions, and is generally poorly transcribed in high-oxygen environments such as the oxic surface waters of the tropical North Atlantic[32]. Legume-associated N_2-fixing rhizobia also rely on high-affinity terminal oxidases when growing symbiotically[29], because the plant hosts restrict the oxygen supply to the symbionts to control their growth and optimize nitrogen fixation[33]. The legume hosts also suppress the activity of the AMT-type ammonium transporters of nodulating rhizobia, to prevent the uptake of ammonium by the bacteria and to enhance ammonium transfer to the plant[30]. The lack of AMT transporters in *Ca*. T. diatomicola would similarly maximize the transfer of ammonia to the *Haslea* host. *Ca*. T. diatomicola seems to lack the capacity for de novo biosynthesis of some essential amino acids (aromatic amino acids, histidine and proline) and vitamins (for example, biotin and thiamine; Supplementary Table 1), a trait also found in nodulating Rhizobiales that are dependent on their plant host for these essential compounds[34,35]. Together, these results indicate that, similarly to nodulating rhizobia in legume symbioses, growth and N_2 fixation by *Ca*. T. diatomicola is tightly regulated by its host.

To confirm that *Ca*. T. diatomicola fixes N_2, we measured the assimilation of ^{15}N from $^{15}N_2$ in individual *Ca*. T. diatomicola–*Haslea* symbioses using nanoscale secondary ion mass spectrometry (nanoSIMS). All investigated *Ca*. T. diatomicola cells fixed $^{15}N_2$ and more than 99% of the fixed nitrogen was subsequently transferred to the diatom host, which is likely to have been facilitated by the lack of AMT transporters in *Ca*. T. diatomicola (Fig. 3a,c). As such, the symbiont fixed 100-fold more nitrogen than would be needed for its own growth, which is similar to previous reports for N_2-fixing cyanobacteria–diatom symbioses[26].

Single-cell uptake of ^{13}C carbon from $^{13}CO_2$, measured simultaneously with N_2 fixation, revealed that the photosynthetic diatom in return transferred around 1% of fixed carbon to the symbiont for growth (Fig. 3b,c). The carbon supplied by the diatom might also be stored as glycogen, lipids or Calvin–Benson–Bassham-cycle products, as indicated by the carbon-rich biomass of the symbiont relative to the diatom host (Extended Data Fig. 7). Similar to nodulating rhizobia, *Ca*. T. diatomicola might store reduced carbon compounds to regulate its carbon flux and act as reductant storage[30]. Furthermore, on the basis of the similar ^{13}C enrichments, both *Ca*. T. diatomicola and the *Haslea* host have comparable carbon-based growth rates (0.6 ± 0.3 and 0.8 ± 0.1 divisions per day (mean ± s.d.), respectively; Fig. 3d). When considered together with microscopic observations of dividing *Ca*. T. diatomicola–*Haslea* symbioses, this indicates the coordinated division of the symbiotic partners and vertical transmission of the symbiont (Extended Data Fig. 4a–d). Such an intricate coordination between host and symbiont growth is required for the long-term persistence and stability of a symbiosis[36]. Moreover, the fast growth of the rhizobia–diatom symbioses (mean, around 0.8 d^{-1}; Extended Data Table 1) relative to the

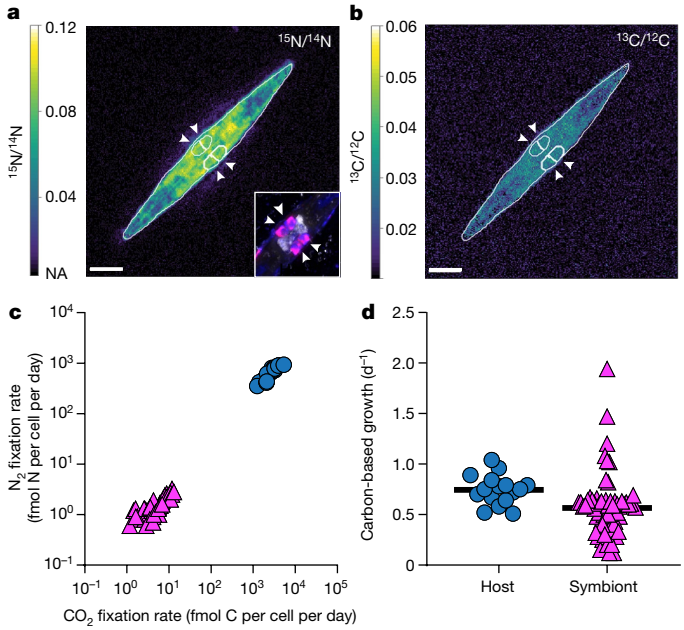

Fig. 3 | Activity of the *Candidatus* Tectiglobus diatomicola symbiont and its diatom host. a,**b**, NanoSIMS images showing the enrichment in ^{15}N from $^{15}N_2$ fixation (**a**) and ^{13}C from $^{13}CO_2$ fixation (**b**). The inset shows the corresponding fluorescence image after hybridization of *Ca*. T. diatomicola cells (indicated by white arrowheads) with specific oligonucleotide probes (in pink, overlay of Hypho638–Hypho825 mix in blue and Hypho1147 in red, respectively) (Extended Data Table 2). Scale bars, 5 µm. **c**, Cellular CO_2 and N_2 fixation rates of *Ca*. T. diatomicola symbionts (pink triangles, $n = 64$) and their diatom hosts (blue circles, $n = 16$). **d**, Carbon-based growth rates of symbionts (pink triangles, $n = 64$) and hosts (blue circles, $n = 16$) (black lines indicate mean; see Methods).

cyanobacteria–diatom symbioses (mean, around 0.2 d^{-1}; Extended Data Table 1) suggests that *Ca*. T. diatomicola might contribute substantially to the nitrogen input to the oligotrophic tropical North Atlantic.

Ecological and evolutionary implications

To assess the relative importance of the *Ca*. T. diatomicola–*Haslea* symbiosis for N_2 fixation in surface waters of the tropical North Atlantic, we calculated their total N_2 fixation activity on the basis of their cellular N_2 fixation rates and abundance. Owing to the large transfer of nitrogen from the *Ca*. T. diatomicola symbiont to its host diatom (Fig. 3a,c), the biomass of both *Ca*. T. diatomicola and its *Haslea* host was considered for calculations (see Supplementary Methods). On average, N_2 fixation rates for the *Ca*. T. diatomicola–*Haslea* symbiosis were around 650 fmol N d^{-1}, which equates to around 1.5 nmol N l^{-1} d^{-1} on the basis of its in situ abundance (around 2,000 cells per litre; Extended Data Table 1). This is comparable to the combined contribution of the most abundant cyanobacteria–diatom symbioses that we observed in these waters: the cyanobacterium *Richelia*, which associates with the diatoms *Hemiaulus* and *Guinardia* (around 1.6 nmol N l^{-1} d^{-1}; Extended Data Table 1). Moreover, N_2 fixation by the *Ca*. T. diatomicola–*Haslea* symbiosis is in the same range of N_2 fixation previously reported from this region for the most abundant cyanobacterial N_2 fixers *Trichodesmium* and UCYN-A (up to 4 and 1.5 nmol N l^{-1} d^{-1}, respectively)[10]. To our knowledge, our nanoSIMS measurements present the first direct quantitative results showing that non-cyanobacterial heterotrophic N_2 fixers fix nitrogen in situ at rates that can account for a substantial part of the high N_2 fixation in the tropical North Atlantic.

To investigate the global distribution of this symbiosis, we retrieved sequences related to *Ca*. T. diatomicola from our own and previously published metagenomes, as well as *nifH* abundances from compilations of quantitative PCR (qPCR) data[8]. These analyses revealed that *Ca*. T. diatomicola is widespread and present in all major oligotrophic ocean regions (Fig. 4a). Notably, our metagenomic data revealed the presence of the *Ca*. T. diatomicola symbiont in regions where gamma-A was previously not reported, such as the oligotrophic South Pacific, Indian and South Atlantic Oceans. In many of these oligotrophic regions, cyanobacterial N_2 fixers are rare[8] and thus cannot account for the measured N_2 fixation. We hypothesize that part of this missing nitrogen is provided by the *Ca*. T. diatomicola symbiosis. Furthermore, genomic evidence suggests that the closest relative of *Ca*. T. diatomicola, *Ca*. T. profundi, is also a widespread heterotrophic N_2-fixing symbiont (Fig. 4a, Extended Data Figs. 3 and 8 and Supplementary Methods). A global-scale metagenomic survey[5] indicates that heterotrophic N_2 fixers are more common than N_2-fixing cyanobacteria in large parts of the surface ocean (Fig. 4b). Although the contribution of these heterotrophs to oceanic N_2 fixation remains unclear, it is noteworthy that they were frequently retrieved from the large size fraction[5] (greater than 3 µm; Extended Data Fig. 1a), suggesting possible host association. Hence, it might be common for N_2-fixing heterotrophs to form obligate or facultative symbioses with diatoms or other unicellular algae. By living in symbiosis with photosynthetic hosts, heterotrophic N_2 fixers would directly fuel CO_2 drawdown and thus contribute to oceanic carbon sequestration.

Ca. T. diatomicola and probably *Ca*. T. profundi represent the first host-associated members of the family *Hyphomicrobiaceae*, as well as the first marine beneficial N_2-fixing symbionts within the order Rhizobiales. Moreover, the finding that rhizobial N_2 fixers can form tight symbioses with unicellular algae expands the known photosynthetic hosts for Rhizobiales beyond the well-described rhizobia–legume symbiosis[17,18]. Besides *Ca*. T. diatomicola and *Ca*. T. profundi, nine other members of the *Hyphomicrobiaceae* were found to have the genomic capacity to fix N_2, eight of which contain *nif* genes that are of alphaproteobacterial origin (Extended Data Figs. 2 and 3). The alphaproteobacterial *nifH*, *nifD*, *nifK*, *nifE*, *nifN*, *nifB* and *nifS* gene sequences from these eight *Hyphomicrobiaceae* form deeply branching sister clades to two of the major nodulating Rhizobiales *nif* clusters (the *Allorhizobium–Mesorhizobium–Rhizobium–Sinorhizobium* and the *Bradyrhizobium* clusters; Extended Data Fig. 2b). The prevalence of *nif* genes throughout the *Hyphomicrobiaceae* family indicates that their last common ancestor was capable of N_2 fixation. This trait was subsequently lost in some members and the ancestor of *Ca*. T. diatomicola and *Ca*. T. profundi is likely to have re-acquired the capacity to fix N_2 through horizontal gene transfer from a gammaproteobacterial donor. Such loss and subsequent re-acquisition of N_2 fixation capacity also occurred during the evolution of the nodulating Rhizobiales[17,18].

Because the *Hyphomicrobiaceae* evolved more than 1,000 million years ago, well before nodulating Rhizobiales lineages began to form symbioses with legume plants around 100 million years ago[17,18], we speculate that beneficial N_2-fixing symbioses in the Rhizobiales order evolved independently in marine environments much earlier than the nodulating species on land. Although *Ca*. T. diatomicola and the nodulating Rhizobiales evolved from one common ancestor and have similar metabolic interactions with their hosts, different degrees of host dependency have resulted in different evolutionary genome adaptations. The terrestrial nodulating rhizobial lineages form facultative symbioses with their host, and have undergone genome expansion to accommodate both a free-living and an intracellular lifestyle[18]. By contrast, the marine *Ca*. T. diatomicola has strongly reduced its genome size, in line with its proposed obligate symbiotic lifestyle. As such, the evolutionary adaptations of *Ca*. T. diatomicola are similar to those of the endosymbiotic cyanobacterium UCYN-A, which functions as an early-stage N_2-fixing organelle[37]. It is tempting to speculate that *Ca*. T. diatomicola, which fulfils the same function in diatoms as UCYN-A does

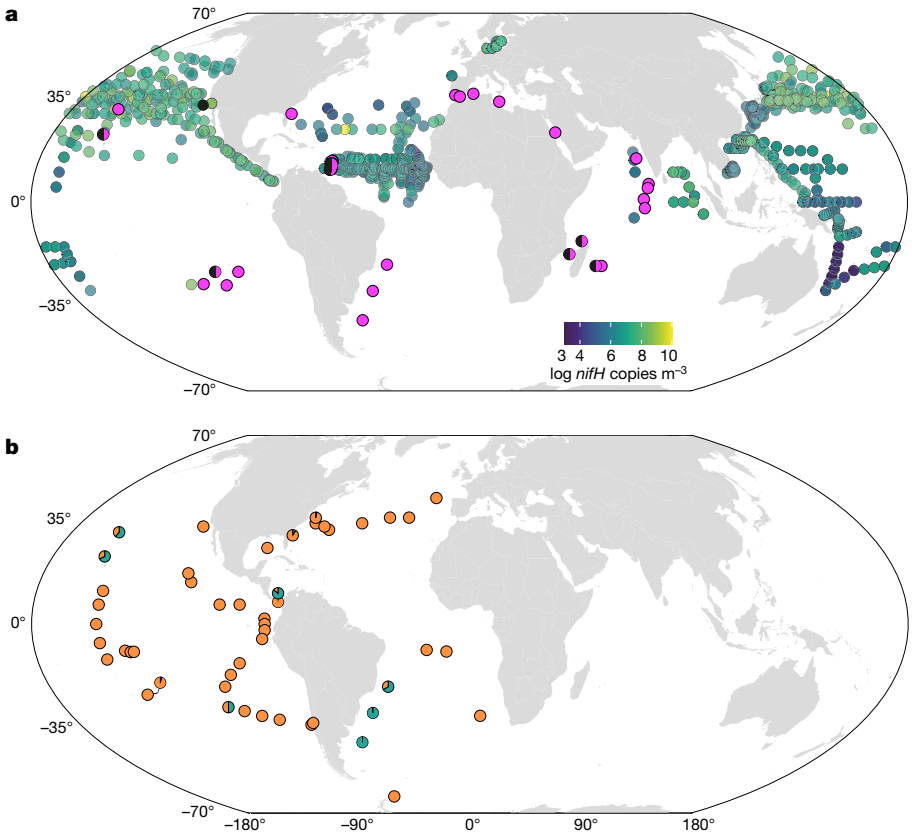

Fig. 4 | Distribution of *Candidatus* Tectiglobus diatomicola and other N_2 fixers in the world's oceans. a, Distribution of *Ca*. T. diatomicola (pink circles) and *Ca*. T. profundi (black circles) based on read detection in metagenome datasets from Tara Oceans and our own samples (see Methods and Supplementary Table 4). Black-and-pink circles are metagenomes in which both *Ca*. Tectiglobus species were detected. The abundance of *Ca*. T. diatomicola on the basis of gamma-A-specific *nifH* qPCR data is shown (circles in blue-to-yellow gradient; data from a previous study[8]). Sample locations in which gamma-A *nifH* qPCR counts were zero are shown in Extended Data Fig. 5b. **b**, Proportion of heterotrophic (orange) versus cyanobacterial (cyan) N_2 fixers identified in a previous study[5] (0.8–2,000 µm size fraction) in metagenome datasets from Tara Oceans.

in haptophyte algae, is also in the early stages of becoming an N_2-fixing organelle. This raises the possibility that endosymbiosis-derived N_2-fixing organelles have originated not only from the cyanobacteria, but also from the Rhizobiales.

Nitrogen-fixing symbiotic Rhizobiales are crucial players in terrestrial productivity; they enable legumes to produce biomass through photosynthesis and consequently provide 20% of the proteins in food production (ref. 7 and references therein). Our results show that symbiotic marine N_2-fixing Rhizobiales, such as *Ca*. T. diatomicola, are major contributors to oceanic N_2 fixation and have a crucial role in sustaining marine productivity and global CO_2 sequestration.

Online content

Any methods, additional references, Nature Portfolio reporting summaries, source data, extended data, supplementary information, acknowledgements, peer review information; details of author contributions and competing interests; and statements of data and code availability are available at https://doi.org/10.1038/s41586-024-07495-w.

1. Gruber, N. & Galloway, J. N. An Earth-system perspective of the global nitrogen cycle. *Nature* **451**, 293–296 (2008).
2. Wang, W.-L., Moore, J. K., Martiny, A. C. & Primeau, F. W. Convergent estimates of marine nitrogen fixation. *Nature* **566**, 205–211 (2019).
3. Farnelid, H. et al. Nitrogenase gene amplicons from global marine surface waters are dominated by genes of non-cyanobacteria. *PLoS One* **6**, e19223 (2011).
4. Zehr, J. P. & Capone, D. G. Changing perspectives in marine nitrogen fixation. *Science* **368**, eaay9514 (2020).
5. Delmont, T. O. et al. Heterotrophic bacterial diazotrophs are more abundant than their cyanobacterial counterparts in metagenomes covering most of the sunlit ocean. *ISME J.* **16**, 927–936 (2022).
6. Poole, P., Ramachandran, V. & Terpolilli, J. Rhizobia: from saprophytes to endosymbionts. *Nat. Rev. Microbiol.* **16**, 291–303 (2018).
7. Kuypers, M. M. M., Marchant, H. K. & Kartal, B. The microbial nitrogen-cycling network. *Nat. Rev. Microbiol.* **16**, 263–276 (2018).
8. Shao, Z. et al. Global oceanic diazotroph database version 2 and elevated estimate of global oceanic N_2 fixation. *Earth Syst. Sci. Data* **15**, 3673–3709 (2023).
9. Halm, H. et al. Heterotrophic organisms dominate nitrogen fixation in the South Pacific Gyre. *ISME J.* **6**, 1238–1249 (2012).
10. Martínez-Pérez, C. et al. The small unicellular diazotrophic symbiont, UCYN-A, is a key player in the marine nitrogen cycle. *Nat. Microbiol.* **1**, 16163 (2016).
11. Shiozaki, T. et al. Basin scale variability of active diazotrophs and nitrogen fixation in the North Pacific, from the tropics to the subarctic Bering Sea. *Global Biogeochem. Cycles* **31**, 996–1009 (2017).
12. Zehr, J. P., Mellon, M. T. & Zani, S. New nitrogen-fixing microorganisms detected in oligotrophic oceans by amplification of nitrogenase (*nifH*) genes. *Appl. Environ. Microbiol.* **64**, 3444–3450 (1998).
13. Riemann, L., Farnelid, H. & Steward, G. Nitrogenase genes in non-cyanobacterial plankton: prevalence, diversity and regulation in marine waters. *Aquat. Microb. Ecol.* **61**, 235–247 (2010).
14. Langlois, R., Großkopf, T., Mills, M., Takeda, S. & LaRoche, J. Widespread distribution and expression of Gamma A (UMB), an uncultured, diazotrophic, γ-proteobacterial *nifH* phylotype. *PLoS One* **10**, e0128912 (2015).
15. Langlois, R. J., Hümmer, D. & LaRoche, J. Abundances and distributions of the dominant nifH phylotypes in the Northern Atlantic Ocean. *Appl. Environ. Microbiol.* **74**, 1922–1931 (2008).
16. Parks, D. H. et al. A standardized bacterial taxonomy based on genome phylogeny substantially revises the tree of life. *Nat. Biotechnol.* **36**, 996–1004 (2018).
17. Garrido-Oter, R. et al. Modular traits of the rhizobiales root microbiota and their evolutionary relationship with symbiotic rhizobia. *Cell Host Microbe* **24**, 155–167 (2018).
18. Wang, S., Meade, A., Lam, H.-M. & Luo, H. Evolutionary timeline and genomic plasticity underlying the lifestyle diversity in Rhizobiales. *mSystems* **5**, e00438-20 (2020).
19. Koirala, A. & Brözel, V. S. Phylogeny of nitrogenase structural and assembly components reveals new insights into the origin and distribution of nitrogen fixation across bacteria and archaea. *Microorganisms* **9**, 1662 (2021).

20. Bolhuis, H., Severin, I., Confurius-Guns, V., Wollenzien, U. I. A. & Stal, L. J. Horizontal transfer of the nitrogen fixation gene cluster in the cyanobacterium *Microcoleus chthonoplastes*. *ISME J.* **4**, 121–130 (2010).
21. McCutcheon, J. P. & Moran, N. A. Extreme genome reduction in symbiotic bacteria. *Nat. Rev. Microbiol.* **10**, 13–26 (2012).
22. Tripp, H. J. et al. Metabolic streamlining in an open-ocean nitrogen-fixing cyanobacterium. *Nature* **464**, 90–94 (2010).
23. Thompson, A. W. et al. Unicellular cyanobacterium symbiotic with a single-celled eukaryotic alga. *Science* **337**, 1546–1550 (2012).
24. Armbrust, E. V. The life of diatoms in the world's oceans. *Nature* **459**, 185–192 (2009).
25. Sterrenburg, F. A. S., Tiffany, M. A., Hinz, F., Herwig, W. E. & Hargraves, P. E. Seven new species expand the morphological spectrum of *Haslea*. A comparison with *Gyrosigma* and *Pleurosigma* (Bacillariophyta). *Phytotaxa* **207**, 143–162 (2015).
26. Foster, R. A. et al. Nitrogen fixation and transfer in open ocean diatom–cyanobacterial symbioses. *ISME J.* **5**, 1484–1493 (2011).
27. Caputo, A., Nylander, J. A. A. & Foster, R. A. The genetic diversity and evolution of diatom-diazotroph associations highlights traits favoring symbiont integration. *FEMS Microbiol. Lett.* **366**, fny297 (2019).
28. Schvarcz, C. R. et al. Overlooked and widespread pennate diatom–diazotroph symbioses in the sea. *Nat. Commun.* **13**, 799 (2022).
29. Dixon, R. & Kahn, D. Genetic regulation of biological nitrogen fixation. *Nat. Rev. Microbiol.* **2**, 621–631 (2004).
30. Udvardi, M. & Poole, P. S. Transport and metabolism in legume–rhizobia symbioses. *Annu. Rev. Plant Biol.* **64**, 781–805 (2013).
31. Nieves-Morión, M., Flores, E. & Foster, R. A. Predicting substrate exchange in marine diatom-heterocystous cyanobacteria symbioses. *Environ. Microbiol.* **22**, 2027–2052 (2020).
32. Berg, J. S. et al. How low can they go? Aerobic respiration by microorganisms under apparent anoxia. *FEMS Microbiol. Rev.* **46**, fuac006 (2022).
33. Kiers, E. T., Rousseau, R. A., West, S. A. & Denison, R. F. Host sanctions and the legume–rhizobium mutualism. *Nature* **425**, 78–81 (2003).
34. Dunn, M. F. Key roles of microsymbiont amino acid metabolism in rhizobia–legume interactions. *Crit. Rev. Microbiol.* **41**, 411–451 (2015).
35. Palacios, O. A., Bashan, Y. & de-Bashan, L. E. Proven and potential involvement of vitamins in interactions of plants with plant growth-promoting bacteria—an overview. *Biol. Fertil. Soils* **50**, 415–432 (2014).
36. Davy, S. K., Allemand, D. & Weis, V. M. Cell biology of cnidarian–dinoflagellate symbiosis. *Microbiol. Mol. Biol. Rev.* **76**, 229–261 (2012).
37. Coale, T. H. et al. Nitrogen-fixing organelle in a marine alga. *Science* **384**, 217–222 (2024).

Methods

Etymology of the *Candidatus* taxa

'*Candidatus* Tectiglobus': Tec.ti.glo'bus. L. past part. *tectus*, hidden; L. masc. n. *globus*, a sphere; N.L. masc. n. *Tectiglobus*, a hidden sphere.

'*Candidatus* Tectiglobus diatomicola': di.a.to.mi'co.la. N.L. fem. n. *diatoma*, a diatom; L. suff. *-cola* (from L. masc. or fem. n. *incola*), inhabitant; N.L. masc. n. *diatomicola*, an inhabitant of diatoms.

'*Candidatus* Tectiglobus profundi': pro.fun'di. L. gen. n. *profundi*, from the depth of the sea, referring to the recovery of its genome from a 4,000-m-deep sediment trap.

Sample collection and experimental set-up

Sampling was performed during two parallel cruises on board RV *Maria S. Merian* (cruise MSM89; Bridgetown, Barbados–Bridgetown, Barbados) and RV *Meteor* (cruise M161; Bridgetown, Barbados–Ponta Delgada, Azores, Portugal) in January–February 2020 in the western tropical North Atlantic. Samples were obtained from Niskin rosette samplers equipped with conductivity, temperature and depth (CTD) systems. At each station, CTD casts were performed to obtain surface water (around 10 m) for dawn-to-dawn incubation experiments of CO_2 and N_2 fixation rates using stable isotope tracers. At the beginning of the incubation experiments, subsamples for DNA and RNA sequencing and FISH were taken. Samples for DNA and RNA sequencing were taken by sequential filtration of 10 l of seawater through 10-µm and 3-µm polycarbonate filters (Isopore, 47 mm diameter) followed by two parallel 0.22-µm Sterivex filters (5 l was filtered through each of the two 0.22-µm filters; all filters from Merck). After filtration, filters were flash-frozen in liquid nitrogen and stored at −80 °C until processing. At the end of the approximately 24-h incubation experiments, subsamples for measurements of bulk rate and for FISH and single-cell analyses were taken. On the RV *Meteor* cruise, additional DNA and RNA samples were collected at the end of the approximately 24-h incubation period through sequential size filtration of around 3 l of incubated seawater. Samples for FISH and nanoSIMS were preserved with methanol-free paraformaldehyde solution (1% w/v final concentration) either for around 24 h at 4 °C or for a few hours at 4 °C followed by 0.5 h at room temperature. Preserved samples were subsequently filtered onto polycarbonate filters (Isopore, 0.2 µm pore size, 25 mm diameter); all samples intended for nanoSIMS analyses were filtered onto gold (Au)-coated polycarbonate filters. Filters were subsequently rinsed with ultrapure water (MilliQ), dried and stored at −20 °C until further analyses.

Metagenomic and metatranscriptomic sequencing

Samples from a total of eight stations were selected for DNA and RNA extractions and subsequent long- and short-read metagenomic and metatranscriptomic sequencing. All library preparation steps and sequencing were performed at the Max Planck Genome Centre (http://mpgc.mpipz.mpg.de/home/). See Supplementary Methods for details of samples, DNA and RNA extraction protocols, library preparation for short- and long-read sequencing and quality trimming.

Recovery and annotation of the *Candidatus* Tectiglobus diatomicola genome

The genome of *Ca*. T. diatomicola was reconstructed from a deeply sequenced short-read metagenomic sample (around 315 Gb, 3–10 µm size fraction from surface water after 24 h of incubation, station 4 from the M161 cruise) together with long-read metagenomes from six stations from the MSM89 cruise (all size fractions from surface water before incubations), as follows. Raw metagenomic short reads were trimmed using Trimmomatic[38] v.0.39 (ILLUMINACLIP:TruSeq3-PE.fa:2:30:10, LEADING:3, TRAILING:3, SLIDINGWINDOW:4:15, MINLEN:36) and assembled using MEGAHIT[39] v.1.2.9. To reduce the size of the assembly (33 million contigs, totalling around 17.7 Gb), it was filtered to retain only contigs with a length of more than 2 kb, 25–40% GC content and a coverage of 29–44; the latter two parameters were chosen on the basis of a preliminary reconstruction of the *Ca*. T. diatomicola genome (for further details, see Supplementary Methods). The remaining 8,218 contigs were visualized in anvi'o[40] v.7.1, and those with high similarity to the previously reconstructed *Ca*. T. diatomicola genome were identified using blastn (BLAST+ (ref. 41) v.2.9.0). Using this approach, a tightly clustered group of 189 contigs, most of which matched with contigs of the previously reconstructed *Ca*. T. diatomicola, was identified in anvi'o[40] v.7.1. The 189 contigs were then iteratively extended and refined, and one iteration included the following steps (see 'Code availability'). Long and short metagenomic reads were mapped onto contigs using minimap2 (ref. 42) v.2.22-r1101 ('-ax map-hifi' for long reads and '-ax sr --score-N 2' for short reads) and the sam mapping files were converted into bam format using SAMtools[43] v.1.14 ('samtools view') and filtered to retain only reads that mapped with more than 98% identity (and more than 80% of the read length for short reads only) using CoverM v.0.6.1 (https://github.com/wwood/CoverM). The remaining mapped long and short reads were converted into fasta format using SAMtools[43] v.1.14 ('samtools fasta'). Short-read pairs in which only a single read was mapped were completed using seqkit[44] v.2.3.0. Subsequently, mapped long and short reads were assembled together using SPAdes[45] v.3.15.3 ('--isolate -k 21,33,55,77,99,111', mapped long reads were supplied using '-s' and scaffolds of the previous iteration were supplied using '--trusted-contigs') and the assembled scaffolds were filtered to retain only scaffolds of at least 1 kb. The filtered scaffolds were then used as input for the next iteration. After 23 iterations, the scaffolds were manually inspected and refined using anvi'o[40] v.7.1, resulting in the current *Ca*. T. diatomicola genome. Completeness and redundancy were estimated using CheckM2 (ref. 46) v.0.1.2 and taxonomy was assigned using GTDB-TK[47] v.2.1.0 and the Genome Taxonomy Database (GTDB)[16] v.r214.

The *Ca*. T. diatomicola genome was at first annotated using Prokka[48] v.1.14.6. Additional information about gene functions was sourced from the RAST web server[49] (https://rast.nmpdr.org/) and through DIAMOND[50] v.2.0.8 similarity searches against the KEGG[51] v.58 and eggNOG[52] v.4.5 databases using the utility script 'sqm_annot.pl' from the SqueezeMeta metagenomics pipeline[53] v.1.6.2. The utility script 'sqm_annot.pl' was further used for taxonomic annotation of all coding sequences using a last common ancestor approach[53]. For genes of interest on the *nif* cluster encoding contig, the taxonomic origin was further investigated using phylogenetic analyses and/or by manual inspection of their best blast hits (see Supplementary Methods). Highly transcribed genes (top 20%) were further inspected using the InterPro web server[54] v.95.0-97.0 (https://www.ebi.ac.uk/interpro/result/InterProScan) and searches against the NCBI-nr database[55] using the NCBI BLAST web server (https://blast.ncbi.nlm.nih.gov/Blast.cgi).

Genome comparisons

The gene content of the two *Ca*. Tectiglobus genomes was compared to that of two closely related MAGs (GCA_905480435 and GCA_002689605). The genes for each genome were annotated with COG identifiers using anvi'o[40] v.7.1 (https://merenlab.org/2016/10/25/cog-annotation/) and genes within each COG category were summed. Whole-genome alignment and identification of blocks of conserved regions within the two *Ca*. Tectiglobus genomes were performed using mauve[56] (development snapshot 2015-02-26).

Phylogenetic analyses

A maximum likelihood phylogenetic tree of *Ca*. T. diatomicola, *Ca*. T. profundi and all Rhizobiales and Parvibaculales (outgroup) genomes from the GTDB[16] (v.r214), as well as HBD_Alpha_05 (a marine MAG from the *Hyphomicrobiaceae* family also containing *nif* genes[5]) was calculated on the basis of 16 ribosomal proteins[57], using muscle[58] v.3.8.1551 for alignment and FastTree[59] v.2.1.11 for tree calculation. The resulting

tree was visualized in iToL[60] v.6.8.1. For further details and the phylogeny of marker proteins (NifH, NifD, NifK, NifE, NifN, NifB, NifS and CcoN), see Supplementary Methods.

Candidatus Tectiglobus diatomicola transcriptome analysis

To obtain gene transcription information for *Ca*. T. diatomicola, all sequenced metatranscriptome reads were combined and mapped to the *Ca*. T. diatomicola genome using BWA-MEM[61] v.0.7.17-r1188, and the resulting mapping files were filtered requiring at least 95% sequence identity and at least 80% of the read to align (mapping and filtering were done through CoverM v.0.6.1). Gene counts were generated using featureCounts[62] v.2.0.1 and TPM values for protein-coding genes were calculated as previously described[63]. The genome plot (Fig. 2a) including TPM values was generated using BRIG[64] v.0.95 and DNAPlotter[65] v.18.1.0.

Global abundance of *Candidatus* Tectiglobus diatomicola and *Candidatus* Tectiglobus profundi

To determine the global distribution and abundance of *Ca*. T. diatomicola and *Ca*. T. profundi, we analysed their presence in metagenomes and in publicly available qPCR data. To this end, we used metagenomes from the Tara Oceans campaign (total of 1,241 metagenomes from projects PRJEB4352, PRJEB1787, PRJEB9691 and PRJEB9740) and metagenomes that we obtained from the tropical North Atlantic and the South Pacific gyre (see Supplementary Table 4). The contigs for each of the two genomes were concatenated (not including the regions encoding the rRNA gene clusters to reduce non-specific read recruitment) and metagenomic reads were mapped using bbmap v.38.70 (https://sourceforge.net/projects/bbmap/) with a minimum identity threshold of 90%. We only considered each genome to be present in a metagenome when the breadth of coverage (fraction of the genome covered by at least one read) was close to the expected breadth following a previously reported formula[66]:

Expected breadth = $1 - e^{(-0.883 \times \text{coverage})}$ (Extended Data Fig. 5c,d).

In addition, we downloaded gamma-A (that is, *Ca*. T. diatomicola) *nifH* qPCR data[67] from a previous study[8] (referred to as NCD_gammaA_nifH_gene and NCD_g24774A11_nifH_gene, around 2,500 data points), added a pseudocount of 1 to the *nifH* copy numbers, log-transformed the counts and filtered out all samples with a count value of 0. We then plotted the coordinates of all metagenomes in which either of the two *Ca*. Tectiglobus genomes were detected together with the log-transformed *Ca*. T. diatomicola *nifH* qPCR counts on a world map using R[68] (Fig. 4). qPCR samples in which *Ca*. T. diatomicola (gamma-A) *nifH* had a count value of 0 were plotted separately (Extended Data Fig. 5b).

Software for bioinformatics analyses

Further software that was used during the analysis of the sequencing data that is described in the Supplementary Information: hifiasm-meta[69] v.0.2-r043 for the assembly of long-read metagenomes; CompareM v.0.1.2 (https://github.com/dparks1134/CompareM) for the calculation of average amino acid identity between *Ca*. T. diatomicola and closely related genomes; fastANI[70] v.1.33 for the calculation of average nucleotide identity between preliminary MAGs; USEARCH[71] v.11.0.667 for clustering sequences on the basis of similarity before phylogenetic tree constructions; MAFFT[72] v.7.505 for calculating and trimAl[73] v.1.4.1 for trimming multiple sequence alignments; ModelFinder[74] for predicting best-fitting models; and UFBoot2 (ref. 75) for calculating ultrafast bootstraps during the construction of maximum likelihood trees with IQ-TREE[76] v.2.2.0.3 and v.2.2.2.7. The following software was used as part of the SqueezeMeta metagenomics pipeline[53] v.1.6.2: Barrnap 0.9-dev (https://github.com/tseemann/barrnap) for the prediction of ribosomal RNAs; the RDP classifier[77] v.2.10.2 for the taxonomic classification of predicted 16S rRNA sequences; prodigal[78] v.2.6.3 for gene prediction; HMMER v.3.1b2 (http://hmmer.org/) for HMM homology searches against the Pfam database[79]; Bowtie2 (ref. 80) v.2.3.4.1 for mapping short reads; MetaBAT 2 (ref. 81) v.2.12.1, MaxBin 2.0 (ref. 82) and CONCOCT[83] v1.1.0 for the binning of contigs into MAGs; DAS Tool[84] v.1.1.1 for integrating the results from the three binning tools; and bbduk v38.87 (https://sourceforge.net/projects/bbmap/) for trimming of metatranscriptomic reads.

Bulk rates of CO_2 and N_2 fixation

Rates of CO_2 and N_2 fixation were determined as previously described[10,85] (with a detailed description in the Supplementary Methods). Stable isotope incubations (^{15}N-N_2 and ^{13}C-DIC (dissolved inorganic carbon)) were performed in triplicate for 24 h (dawn to dawn). Bottles were incubated in on-deck incubators continuously flushed with surface seawater, with simulated light conditions[86]. After around 24 h, subsamples were taken for elemental and isotopic biomass analyses as well as FISH and nanoSIMS analyses. Fixation rates were calculated on the basis of the incorporation of ^{13}C and ^{15}N into biomass (that is, the change in isotopic composition) for both bulk and single-cell activities (Supplementary Methods).

Visualization and abundance of *Candidatus* Tectiglobus diatomicola

To visualize the newly identified *Ca*. T. diatomicola, we designed FISH probes targeting the 16S rRNA[87,88] (Supplementary Methods). In total, four FISH probes were designed: two specifically targeting *Ca*. T. diatomicola (Hypho825 and Hypho638) and two with a broader coverage, targeting many members of the *Hyphomicrobiaceae* (Hypho1147) and several members of the *Hyphomicrobiaceae* genera *Hyphomicrobium*, *Filomicrobium* and *Pedomicrobium* (Hypho734) (see Extended Data Table 2 and Supplementary Methods). The optimal formamide concentrations for these new probes were tested using Clone-FISH[89] (Supplementary Methods).

The *Ca*. T. diatomicola cells were visualized using catalysed reporter deposition-FISH (CARD-FISH) with the four new horseradish peroxidase (HRP)-labelled probes either alone or in combination (double hybridization) and together with helpers or competitors to increase signal intensity (Extended Data Table 2). CARD-FISH was performed as previously described[90]. Microscopy was performed using a Zeiss Axio Imager.M2 wide-field epifluorescence microscope equipped with a Zeiss Axiocam 506 mono camera and Zeiss ZEN 3.2 blue edition software, a Zeiss LSM 780 confocal laser scanning microscope equipped with Zeiss Elyra PS.1 super-resolution-structured illumination microscopy and a laser microdissection (LMD) microscope (LMD 7000, Leica). For better identification of the diatom host of *Ca*. T. diatomicola, host diatoms containing FISH-positive cells were visualized by SEM with a FEI Quanta 250 FEG ESEM (Thermo Fisher Scientific, FEI) (see Supplementary Methods). Abundances of the *Ca*. T. diatomicola–*Haslea* symbiosis were determined as the number of diatom hosts containing FISH-positive cells from filter pieces representing around 25 ml of sampled water (Extended Data Table 1).

Abundance of free-living and host-associated cyanobacterial N_2 fixers

Free-living (*Trichodesmium*, *Crocosphaera*) and host-associated (diatom-associated *Richelia*) cyanobacterial N_2 fixers were identified by morphology and chlorophyll *a*- and/or phycoerythrin autofluorescence using an LMD microscope (LMD 7000, Leica). *Richelia* were found associated with the diatoms *Guinardia*, sometimes also referred to as *Rhizosolenia*, and *Hemiaulus*. Abundances were determined as the number of *Richelia*-containing host diatoms. Abundances of *Trichodesmium* were determined by measuring the total (summed) length of all free trichomes, and by dividing the total trichome length by the average cell length. Abundances of *Crocosphaera* cells were determined by direct cell counts. Abundances were determined from whole filters representing around 300–360 ml of sampled water (Extended Data Table 1).

Single-cell N_2-fixation activities using nanoSIMS

Au-sputtered filters from the end of the stable isotope incubations were used for nanoSIMS (nanoSIMS 50L, CAMECA) to measure the single-cell carbon and nitrogen isotopic composition and to determine the single-cell CO_2 and N_2 fixation activities of *Ca*. T. diatomicola and their *Haslea* hosts as well as *Richelia* and their diatom hosts (*Hemiaulus* and *Guinardia*) (Extended Data Table 1). Both target symbioses were visualized as described above and subsequently marked using an LMD microscope (LMD 7000, Leica). NanoSIMS analyses were performed as previously described[90] and details are provided in the Supplementary Methods. The isotopic ratios ($^{13}C/^{12}C$ and $^{12}C^{15}N/^{12}C^{14}N$) of regions of interest were determined by overlaying epifluorescence images of FISH-positive cells and their host diatom (for *Ca*. T. diatomicola–*Haslea* symbiosis) or brightfield and autofluorescence images (diatom-associated *Richelia*) with the nanoSIMS images (secondary electrons). For the elemental imaging (Extended Data Fig. 7), carbon (^{12}C), nitrogen ($^{12}C^{14}N$) and secondary electrons were overlaid; for this image only, background signals were removed. Cellular rates and abundances were combined to determine the absolute contributions of the *Ca*. T. diatomicola–*Haslea* symbiosis and diatom-associated *Richelia* to the bulk N_2 fixation rate as previously described[10]. For both the *Ca*. T. diatomicola–*Haslea* symbiosis and the diatom-associated *Richelia*, the amount of nitrogen recovered in the diatom was also taken into account. Carbon-based growth rates for individual cells as well as whole symbioses were determined using the equation provided in a previous report[10] and mass-balancing host and symbiont. Single-cell activities and contributions in our study can be considered conservative because $^{13}C/^{12}C$ and $^{15}N/^{14}N$ ratios can be diluted during sample preparation, which can lead to underestimation[91–93].

Statistics and reproducibility

For Fig. 1b,c, the correlative SEM and fluorescence (confocal as well as epifluorescence) images are representative of a total of 11 diatoms from surface waters of 3 independent environmental samples. Additional fluorescence images (Fig. 1c) were obtained from a total of 27 diatoms from 6 independent environmental samples.

For Fig. 3a,b, the correlative nanoSIMS images are representative of a total of 16 diatoms (containing a total of 64 symbionts) from 3 independent environmental samples.

For Extended Data Fig. 4, the correlative fluorescence (confocal as well as epifluorescence) and SEM images (Extended Data Fig. 4a–d) are representative of a total of 13 diatoms, which contained more than 4 symbionts, from 5 independent environmental samples. The NON338-probe image (Extended Data Fig. 4e) is representative of a total of 32 diatoms from 3 independent environmental samples; however, chloroplasts were not always visible. Extended Data Fig. 4f, showing *Ca*. T. diatomicola cells after hybridization with a specific oligonucleotide probe in close vicinity to the H-shaped nucleus and bilobed chloroplasts, is representative of a total of 18 diatoms from 3 independent environmental samples. The SEM image showing a whole diatom (Extended Data Fig. 4g) is representative of a total of 19 diatoms from 2 independent environmental samples. Extended Data Fig. 4h–k show a selection of magnified images that helped with the identification of the diatom host.

For Extended Data Fig. 7, one diatom was analysed.

Reporting summary

Further information on research design is available in the Nature Portfolio Reporting Summary linked to this article.

Data availability

Read data from metagenomic analyses pertaining to *Ca*. T. diatomicola have been deposited at the NCBI under BioProject accession number PRJNA1036431, including the MAGs of *Ca*. T. diatomicola and *Ca*. T. profundi under the accession numbers JAZDSJ000000000 and DAWWJP000000000, respectively. RNA-sequencing data can be found under the same BioProject number with the accession numbers SRR26695118, SRR26695119 and SRR26695121–SRR26695130. The publicly available sequences used for phylogenetic tree construction and genome comparison can be found at the GTDB (https://gtdb.ecogenomic.org/) under the accession numbers given in Supplementary Data 1–9 (tree file for each tree). Publicly available MAGs from a previous study[5] can be found at https://figshare.com/articles/dataset/Marine_diazotrophs/14248283. Tara Oceans metagenomes used in this study can be found at https://www.ncbi.nlm.nih.gov/bioproject/173486 with the following BioProject accessions used in this study: PRJEB4352 (size fractions for protists), PRJEB1787 (size fractions for prokaryotes), PRJEB9691 (size fractions for protists from polar circle samples) and PRJEB9740 (size fractions for prokaryotes from polar circle samples). For the reconstruction of the MAG of *Ca*. T. profundi, the metagenomic data that we used can be found at the GTDB (https://gtdb.ecogenomic.org/genome?gid=GCA_013214245.1; original MAG) and at the Sequence Read Archive under https://www.ncbi.nlm.nih.gov/bioproject/PRJNA482655 with the accession numbers SRR7648332, SRR7648341, SRR7648350, SRR7632647 and SRR7648334 (metagenomes used for MAG reconstruction). Publicly available qPCR data from a previous study[8] can be found at https://doi.org/10.6084/m9.figshare.21677687.v3. Additional databases used in this study can found at the following links: eggNOG: http://eggnog45.embl.de/download/eggnog_4.5/data/NOG/; ncbi-nr database: https://ftp.ncbi.nlm.nih.gov/blast/db/FASTA/nr.gz; pfam database: https://www.ebi.ac.uk/interpro/download/pfam/; and kegg database: http://andes.cnb.csic.es/SqueezeMeta/kegg.db.gz. Source data are provided with this paper.

Code availability

Custom scripts for iterative bin refinements are deposited at https://github.com/bresyd/mag_refinement/tree/main.

38. Bolger, A. M., Lohse, M. & Usadel, B. Trimmomatic: a flexible trimmer for Illumina sequence data. *Bioinformatics* **30**, 2114–2120 (2014).
39. Li, D., Liu, C.-M., Luo, R., Sadakane, K. & Lam, T.-W. MEGAHIT: an ultra-fast single-node solution for large and complex metagenomics assembly via succinct de Bruijn graph. *Bioinformatics* **31**, 1674–1676 (2015).
40. Eren, A. M. et al. Community-led, integrated, reproducible multi-omics with anvi'o. *Nat. Microbiol.* **6**, 3–6 (2021).
41. Camacho, C. et al. BLAST+: architecture and applications. *BMC Bioinformatics* **10**, 421 (2009).
42. Li, H. Minimap2: pairwise alignment for nucleotide sequences. *Bioinformatics* **34**, 3094–3100 (2018).
43. Danecek, P. et al. Twelve years of SAMtools and BCFtools. *Gigascience* **10**, giab008 (2021).
44. Shen, W., Le, S., Li, Y. & Hu, F. SeqKit: a cross-platform and ultrafast toolkit for FASTA/Q file manipulation. *PLoS One* **11**, e0163962 (2016).
45. Prjibelski, A., Antipov, D., Meleshko, D., Lapidus, A. & Korobeynikov, A. Using SPAdes de novo assembler. *Curr. Protoc. Bioinformatics* **70**, e102 (2020).
46. Chklovski, A., Parks, D. H., Woodcroft, B. J. & Tyson, G. W. CheckM2: a rapid, scalable and accurate tool for assessing microbial genome quality using machine learning. *Nat. Methods* **20**, 1203–1212 (2023).
47. Chaumeil, P.-A., Mussig, A. J., Hugenholtz, P. & Parks, D. H. GTDB-Tk v2: memory friendly classification with the genome taxonomy database. *Bioinformatics* **38**, 5315–5316 (2022).
48. Seemann, T. Prokka: rapid prokaryotic genome annotation. *Bioinformatics* **30**, 2068–2069 (2014).
49. Aziz, R. K. et al. The RAST server: rapid annotations using subsystems technology. *BMC Genomics* **9**, 75 (2008).
50. Buchfink, B., Reuter, K. & Drost, H.-G. Sensitive protein alignments at tree-of-life scale using DIAMOND. *Nat. Methods* **18**, 366–368 (2021).
51. Kanehisa, M. & Goto, S. KEGG: Kyoto Encyclopedia of Genes and Genomes. *Nucleic Acids Res.* **28**, 27–30 (2000).
52. Huerta-Cepas, J. et al. eggNOG 4.5: a hierarchical orthology framework with improved functional annotations for eukaryotic, prokaryotic and viral sequences. *Nucleic Acids Res.* **44**, D286–D293 (2016).
53. Tamames, J. & Puente-Sánchez, F. SqueezeMeta, a highly portable, fully automatic metagenomic analysis pipeline. *Front. Microbiol.* **9**, 3349 (2019).
54. Paysan-Lafosse, T. et al. InterPro in 2022. *Nucleic Acids Res.* **51**, D418–D427 (2023).
55. Benson, D. A., Karsch-Mizrachi, I., Lipman, D. J., Ostell, J., & Wheeler, D. L. GenBank. *Nucleic Acids Res.* **33**, D34–D38 (2005).

56. Darling, A. C. E., Mau, B., Blattner, F. R. & Perna, N. T. Mauve: multiple alignment of conserved genomic sequence with rearrangements. *Genome Res.* **14**, 1394–1403 (2004).
57. Hug, L. A. et al. A new view of the tree of life. *Nat. Microbiol.* **1**, 16048 (2016).
58. Edgar, R. C. MUSCLE: multiple sequence alignment with high accuracy and high throughput. *Nucleic Acids Res.* **32**, 1792–1797 (2004).
59. Price, M. N., Dehal, P. S. & Arkin, A. P. FastTree 2—approximately maximum-likelihood trees for large alignments. *PLoS One* **5**, e9490 (2010).
60. Letunic, I. & Bork, P. Interactive Tree Of Life (iTOL) v5: an online tool for phylogenetic tree display and annotation. *Nucleic Acids Res.* **49**, W293–W296 (2021).
61. Li, H. Aligning sequence reads, clone sequences and assembly contigs with BWA-MEM. Preprint at *arXiv* https://doi.org/10.48550/arXiv.1303.3997 (2013).
62. Liao, Y., Smyth, G. K. & Shi, W. featureCounts: an efficient general purpose program for assigning sequence reads to genomic features. *Bioinformatics* **30**, 923–930 (2014).
63. Zhao, S., Ye, Z. & Stanton, R. Misuse of RPKM or TPM normalization when comparing across samples and sequencing protocols. *RNA* **26**, 903–909 (2020).
64. Alikhan, N.-F., Petty, N. K., Ben Zakour, N. L. & Beatson, S. A. BLAST Ring Image Generator (BRIG): simple prokaryote genome comparisons. *BMC Genomics* **12**, 402 (2011).
65. Carver, T., Thomson, N., Bleasby, A., Berriman, M. & Parkhill, J. DNAPlotter: circular and linear interactive genome visualization. *Bioinformatics* **25**, 119–120 (2009).
66. Olm, M. R. et al. inStrain profiles population microdiversity from metagenomic data and sensitively detects shared microbial strains. *Nat. Biotechnol.* **39**, 727–736 (2021).
67. Shao, Z. et al. Version 2 of the global ocean diazotroph database. Figshare https://doi.org/10.6084/m9.figshare.21677687.v3 (2023).
68. R Core Team. *R: A Language and Environment for Statistical Computing*. http://www.R-project.org/ (R Foundation for Statistical Computing, 2020).
69. Feng, X., Cheng, H., Portik, D. & Li, H. Metagenome assembly of high-fidelity long reads with hifiasm-meta. *Nat. Methods* **19**, 671–674 (2022).
70. Jain, C., Rodriguez-R, L. M., Phillippy, A. M., Konstantinidis, K. T. & Aluru, S. High throughput ANI analysis of 90K prokaryotic genomes reveals clear species boundaries. *Nat. Commun.* **9**, 5114 (2018).
71. Edgar, R. C. Search and clustering orders of magnitude faster than BLAST. *Bioinformatics* **26**, 2460–2461 (2010).
72. Katoh, K. & Standley, D. M. MAFFT multiple sequence alignment software version 7: improvements in performance and usability. *Mol. Biol. Evol.* **30**, 772–780 (2013).
73. Capella-Gutiérrez, S., Silla-Martínez, J. M. & Gabaldón, T. trimAl: a tool for automated alignment trimming in large-scale phylogenetic analyses. *Bioinformatics* **25**, 1972–1973 (2009).
74. Kalyaanamoorthy, S., Minh, B. Q., Wong, T. K. F., von Haeseler, A. & Jermiin, L. S. ModelFinder: fast model selection for accurate phylogenetic estimates. *Nat. Methods* **14**, 587–589 (2017).
75. Hoang, D. T., Chernomor, O., von Haeseler, A., Minh, B. Q. & Vinh, L. S. UFBoot2: improving the ultrafast bootstrap approximation. *Mol. Biol. Evol.* **35**, 518–522 (2018).
76. Minh, B. Q. et al. IQ-TREE 2: new models and efficient methods for phylogenetic inference in the genomic era. *Mol. Biol. Evol.* **37**, 1530–1534 (2020).
77. Wang, Q., Garrity, G. M., Tiedje, J. M. & Cole, J. R. Naive Bayesian classifier for rapid assignment of rRNA sequences into the new bacterial taxonomy. *Appl. Environ. Microbiol.* **73**, 5261–5267 (2007).
78. Hyatt, D. et al. Prodigal: prokaryotic gene recognition and translation initiation site identification. *BMC Bioinformatics* **11**, 119 (2010).
79. Finn, R. D. et al. The Pfam protein families database: towards a more sustainable future. *Nucleic Acids Res.* **44**, D279–D285 (2016).
80. Langmead, B. & Salzberg, S. L. Fast gapped-read alignment with Bowtie 2. *Nat. Methods* **9**, 357–359 (2012).
81. Kang, D. D. et al. MetaBAT 2: an adaptive binning algorithm for robust and efficient genome reconstruction from metagenome assemblies. *PeerJ.* **7**, e7359 (2019).
82. Wu, Y.-W., Simmons, B. A. & Singer, S. W. MaxBin 2.0: an automated binning algorithm to recover genomes from multiple metagenomic datasets. *Bioinformatics* **32**, 605–607 (2016).
83. Alneberg, J. et al. Binning metagenomic contigs by coverage and composition. *Nat. Methods* **11**, 1144–1146 (2014).
84. Sieber, C. M. K. et al. Recovery of genomes from metagenomes via a dereplication, aggregation and scoring strategy. *Nat. Microbiol.* **3**, 836–843 (2018).
85. Großkopf, T. et al. Doubling of marine dinitrogen-fixation rates based on direct measurements. *Nature* **488**, 361–364 (2012).
86. Duerschlag, J. et al. Niche partitioning by photosynthetic plankton as a driver of CO_2-fixation across the oligotrophic South Pacific Subtropical Ocean. *ISME J.* **16**, 465–476 (2022).
87. Kitzinger, K. et al. Single cell analyses reveal contrasting life strategies of the two main nitrifiers in the ocean. *Nat. Commun.* **11**, 767 (2020).
88. Graf, J. S. et al. Anaerobic endosymbiont generates energy for ciliate host by denitrification. *Nature* **591**, 445–450 (2021).
89. Schramm, A., Fuchs, B. M., Nielsen, J. L., Tonolla, M. & Stahl, D. A. Fluorescence in situ hybridization of 16S rRNA gene clones (Clone-FISH) for probe validation and screening of clone libraries. *Environ. Microbiol.* **4**, 713–720 (2002).
90. Kitzinger, K. et al. in *Fluorescence In-Situ Hybridization (FISH) for Microbial Cells: Methods and Concepts* (eds Azevedo, N. F. & Almeida, C.) 207–224 (Springer, 2021).
91. Musat, N. et al. The effect of FISH and CARD-FISH on the isotopic composition of ^{13}C- and ^{15}N-labeled *Pseudomonas putida* cells measured by nanoSIMS. *Syst. Appl. Microbiol.* **37**, 267–276 (2014).
92. Woebken, D. et al. Revisiting N_2 fixation in Guerrero Negro intertidal microbial mats with a functional single-cell approach. *ISME J.* **9**, 485–496 (2015).
93. Meyer, N. R., Fortney, J. L. & Dekas, A. E. NanoSIMS sample preparation decreases isotope enrichment: magnitude, variability and implications for single-cell rates of microbial activity. *Environ. Microbiol.* **23**, 81–98 (2021).
94. Sargent, E. C. et al. Evidence for polyploidy in the globally important diazotroph *Trichodesmium*. *FEMS Microbiol. Lett.* **363**, fnw244 (2016).
95. Bench, S. R., Ilikchyan, I. N., Tripp, H. J. & Zehr, J. P. Two strains of *Crocosphaera watsonii* with highly conserved genomes are distinguished by strain-specific features. *Front. Microbiol.* **2**, 261 (2011).
96. Vernette, C. et al. The Ocean barcode atlas: a web service to explore the biodiversity and biogeography of marine organisms. *Mol. Ecol. Resour.* **21**, 1347–1358 (2021).

Acknowledgements We thank the Leitstelle Deutsche Forschungsschiffe of the German National Research Foundation (DFG) and the captains, crews and chief scientists J. Karstensen, G. Lavik and S. Kinne of the RV *Maria S. Merian* MSM89 and RV *Meteor* M161 cruises for their support; the Ministry of Foreign Affairs and Foreign Trade in Barbados and the Ministry of Foreign and CARICOM Affairs of the Republic of Trinidad and Tobago for permissions to conduct marine scientific research in territorial waters; B. Stevens and S. Bony for coordinating the EUREC^{4}A^{++} project; D. Baranowski and his CTD team for help with sampling; M. Knutzen, G. Klockgether, S. Lilienthal, K. Imhoff, S. Piosek and N. Rujanski for technical support; P. Kociolek and L. Nicolas-Asselineau for advice on diatom taxonomy and phylogenomics, respectively; and A. Oren for his help with the etymology of *Ca*. T. diatomicola and *Ca*. T. profundi. The MSM89 and M161 cruises were financially supported by the DFG (funding numbers: GPF18-2-50 and GPF18-1-69, EUREC^{4}A^{++}) and the Bundesministerium für Bildung und Forschung. This study was funded by the Max Planck Society.

Author contributions B.T., D.R.S. and S. Li processed and analysed all metagenomic and metatranscriptomic data. B.T., M.P., A.T.K. and W.M. performed ship-board sampling and experiments and analysed bulk rate data. M.P. and K.K. designed the FISH probes. D.T. and M.E. performed FISH and microscopy. A.T.K. performed nanoSIMS analyses. S. Littmann performed SEM. A.K. identified and characterized the diatom host. B.T., W.M. and M.M.M.K. designed the study. B.T., H.K.M., B.K., J.M., W.M. and M.M.M.K. wrote the manuscript with contributions from all coauthors.

Funding Open access funding provided by Max Planck Society.

Competing interests The authors declare no competing interests.

Additional information

Supplementary information The online version contains supplementary material available at https://doi.org/10.1038/s41586-024-07495-w.

Correspondence and requests for materials should be addressed to Marcel M. M. Kuypers.

Peer review information *Nature* thanks Douglas Capone, Tom O. Delmont and Philip Poole for their contribution to the peer review of this work.

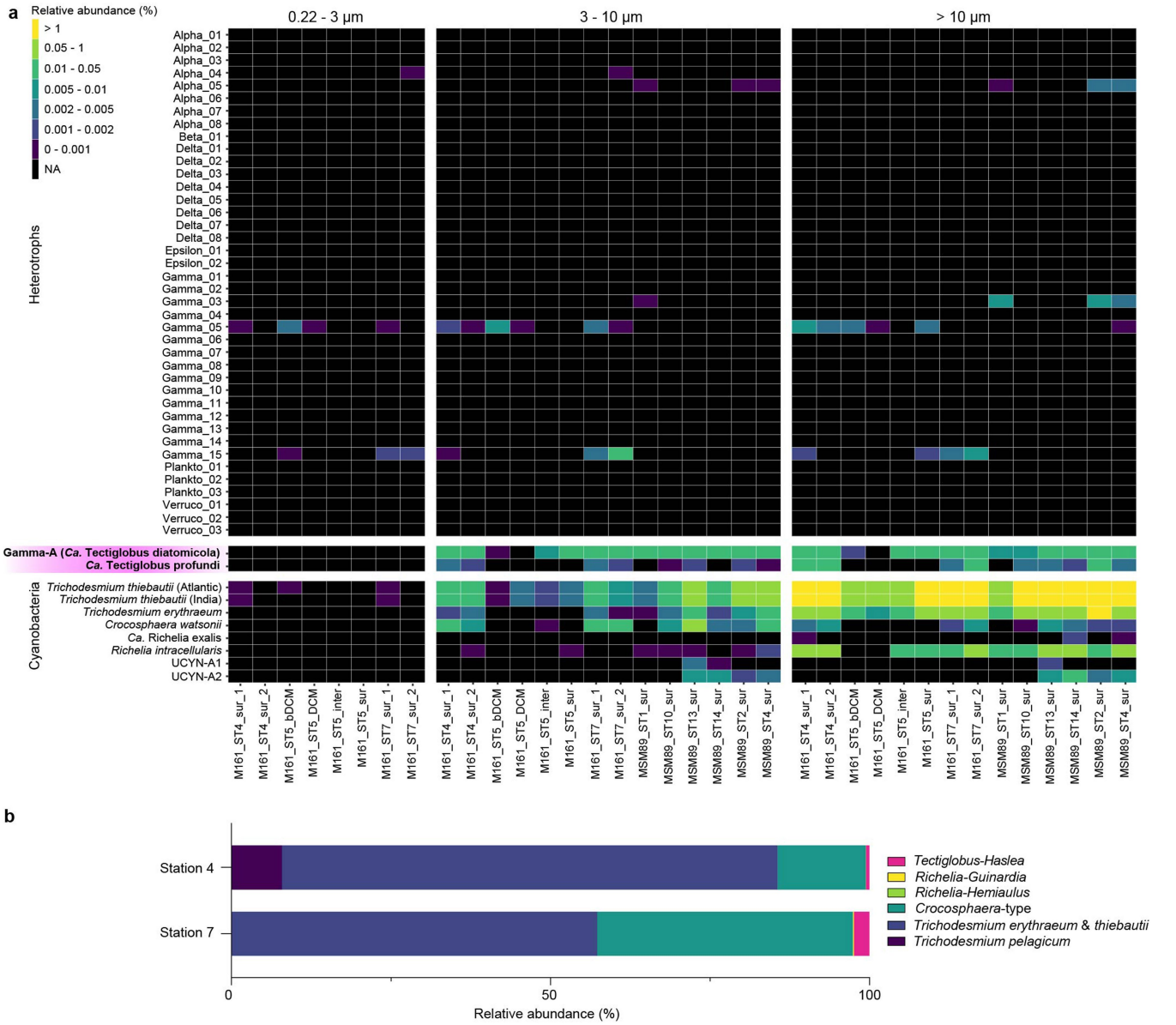

Extended Data Fig. 1 | Relative abundance of heterotrophic and cyanobacterial N_2 fixers in the tropical North Atlantic. a, Relative abundance of '*Ca*. T. diatomicola' (gamma-A), '*Ca*. T. profundi', as well as selected cosmopolitan heterotrophic and cyanobacterial N_2 fixers[5] based on read detection in metagenome data from different size fractions from the tropical North Atlantic. Note that only few known heterotrophic N_2 fixers were detected in the dataset, and that '*Ca*. T. diatomicola' had the highest relative abundance. **b**, Relative abundance of the most abundant known N_2 fixers determined from direct microscopy counts (surface waters of stations 4 and 7 from cruise M161 in the tropical North Atlantic). Note that the metagenome based relative abundances of *Trichodesmium* in the large size fraction overestimate its microscopy-based abundance by an order of magnitude, most likely due to the polyploidy of this genus[94]. By contrast, metagenome based relative abundances of *Crocosphaera* in the large size fraction underestimate its microscopy-based abundance, most likely due to DNA extraction biases[95].

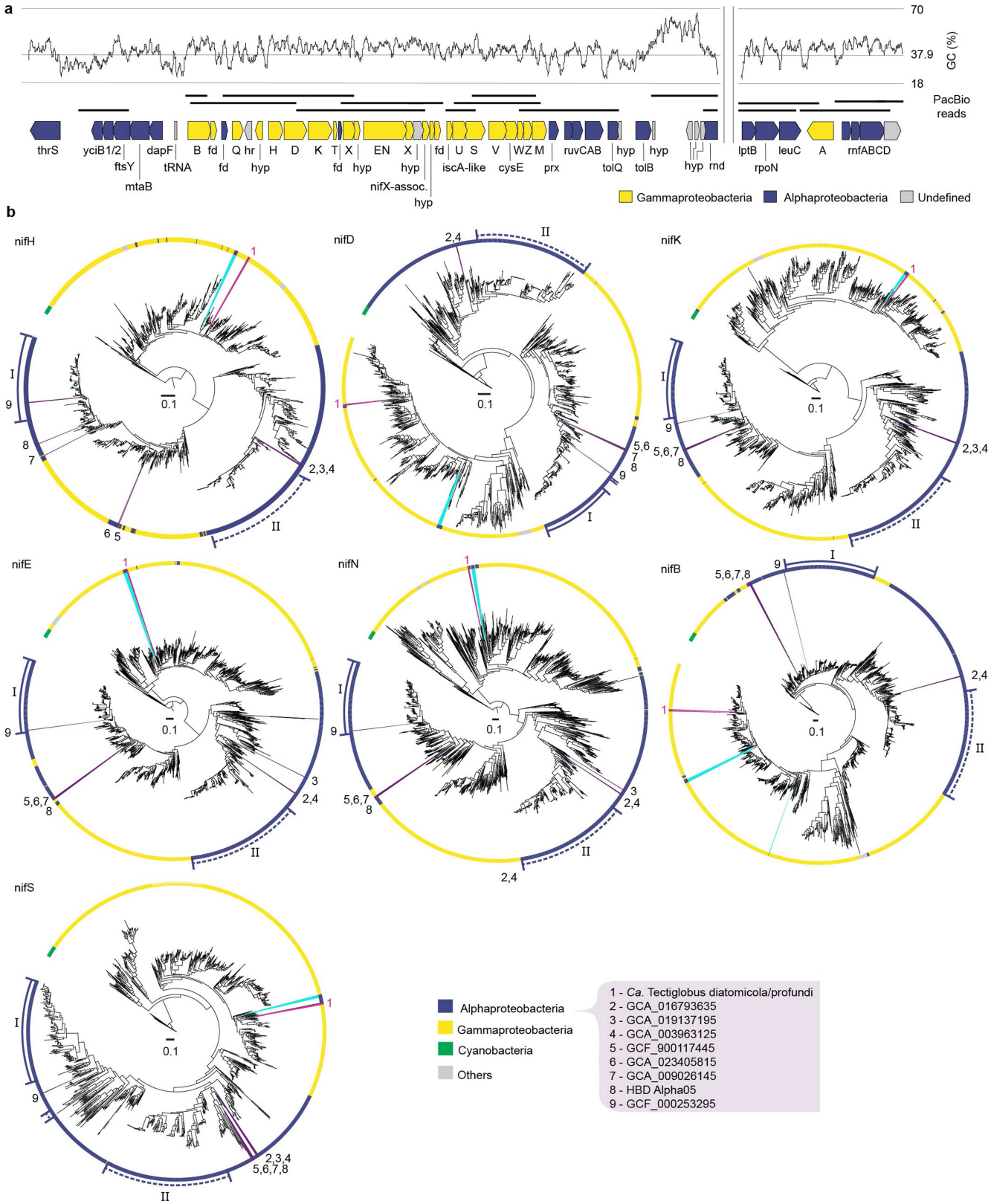

Extended Data Fig. 2 | See next page for caption.

Extended Data Fig. 2 | Organization and phylogeny of nitrogen fixation (*nif*) genes in '*Candidatus* Tectiglobus diatomicola'. a, Organization of the *nif* regulon showing the phylogenetic affiliation and GC content of each gene. All *nif* genes are affiliated to gammaproteobacteria (yellow), whereas almost all other genes in and around the *nif* regulon are affiliated to alphaproteobacteria (blue). The presence of *nifV* indicates that unlike most nodulating rhizobia, '*Ca*. T. diatomicola' has the capacity to synthesize homocitrate, a ligand of the FeMo cofactor[6]. Genes affiliated to gamma-and alphaproteobacteria were found together on individual PacBio reads (solid black lines). Note that there is no substantial difference in GC content between genes of gamma- and alphaproteobacterial origin. **b**, Maximum likelihood phylogenetic trees of NifHDKENBS sequences of the *Pseudomonadota*. Phylogeny is based on the alignment of full-length amino acid sequences retrieved from the GTDB. Cyanobacterial Nif sequences were used as outgroups. All '*Ca*. Tectiglobus diatomicola'/'*Ca*. Tectiglobus profundi' (pink line; 1) Nif protein sequences cluster with gammaproteobacterial sequences, while Nif sequences from other members of the *Hyphomicrobiaceae* family (purple lines; 2–9; Extended Data Fig. 3) cluster with alphaproteobacteria. These alphaproteobacterial Nif protein sequences form deeply branching sister clades to two of the major nodulating Rhizobiales *nif* clusters; i.e. *Bradyrhizobium* (I, solid line) and *Allorhizobium-Mesorhizobium-Rhizobium-Sinorhizobium* (II, dashed line). Note that some other *Rhizobiales* (turquoise lines; members of the *Rhodobiaceae*, *Rhizobiaceae*, *Cohaesibacteraceae* and BM303 families) Nif protein sequences also cluster with the gammaproteobacterial sequences indicating that they were also obtained via horizontal gene transfer from a (common) gammaproteobacterial donor. Tree scales indicate amino acid substitutions per site. Note that in panel A, individual *nif* genes are indicated by capital letters; fd, ferredoxin; hr, hemerythrin; hyp, hypothetical protein; prx, peroxiredoxin; rnd, ribonuclease D.

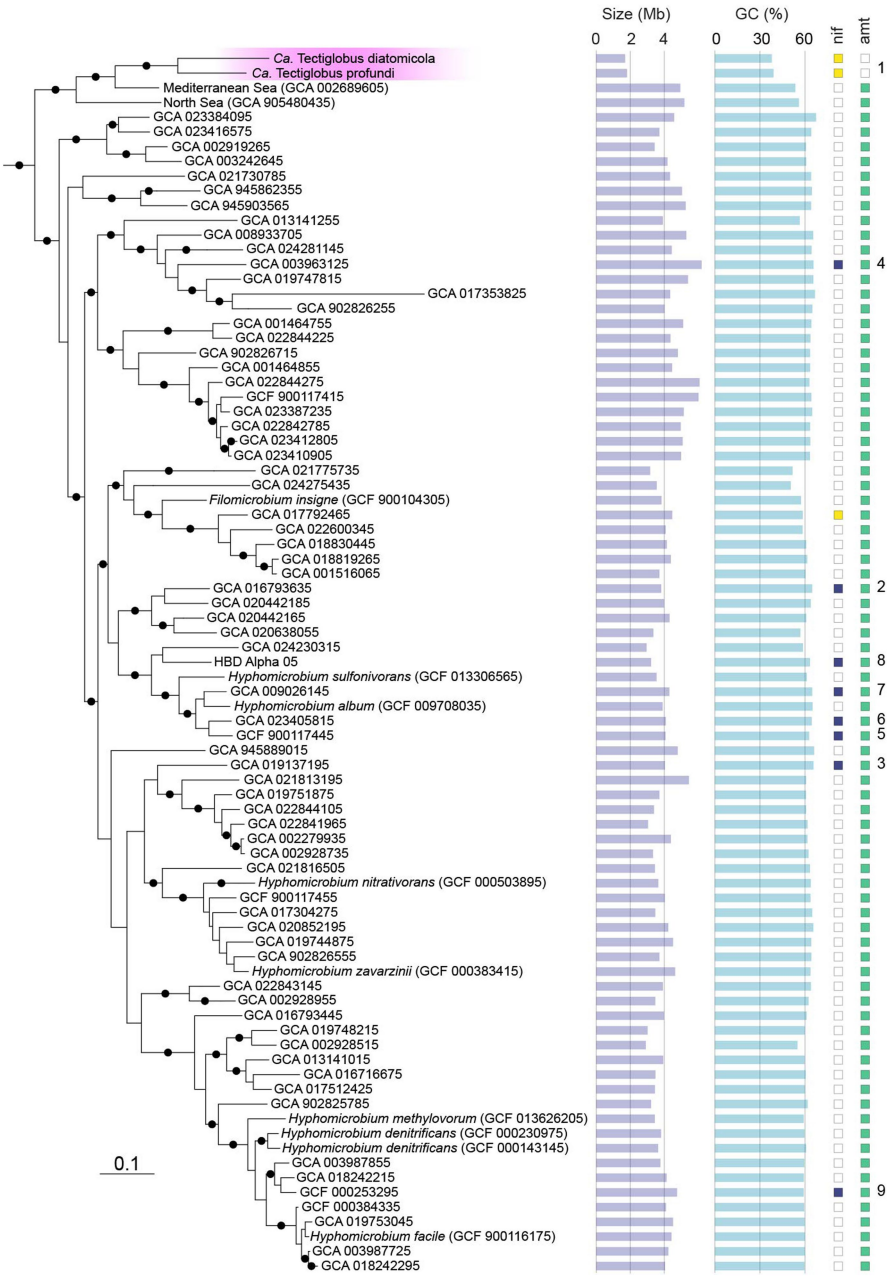

Extended Data Fig. 3 | Maximum likelihood phylogenetic tree of concatenated bacterial marker genes, highlighting genomic features of the *Hyphomicrobiaceae* family. Columns from left to right represent genome size (Mb), GC content (%), presence and phylogeny of *nifH* genes (yellow, gammaproteobacteria; blue, alphaproteobacteria), and presence (green) of ammonium transporter genes (*amt*). The numbers on the right indicate the *nif*-containing members of the *Hyphomicrobiaceae* from Extended Data Fig. 2. '*Ca*. T. diatomicola' and '*Ca*. T. profundi' are highlighted in pink. Only genomes with >80% completion are shown. Black dots indicate >95% bootstrap support. Scale bar indicates amino acid substitutions per site.

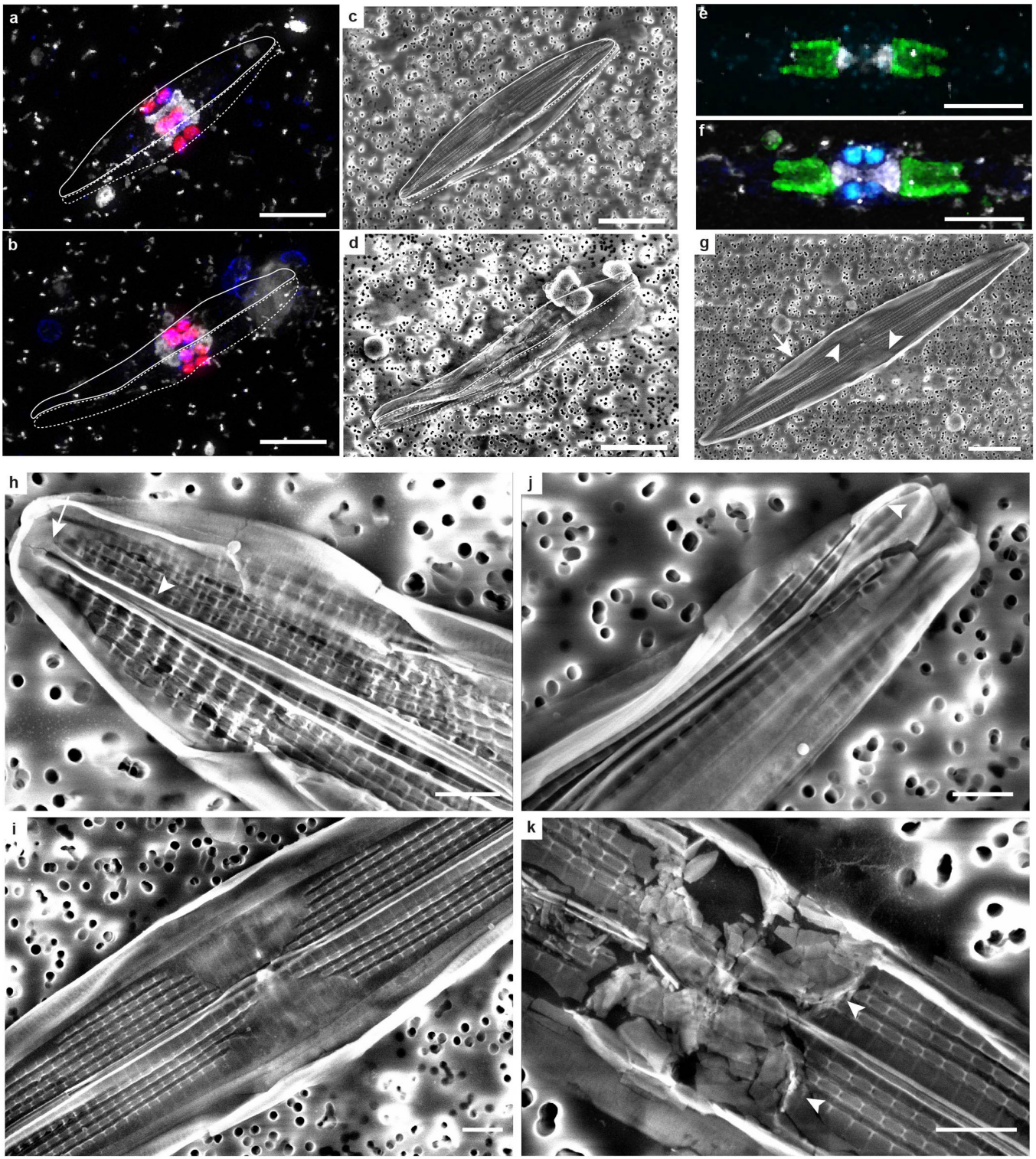

Extended Data Fig. 4 | See next page for caption.

Extended Data Fig. 4 | Microscopic characterization of '*Candidatus* Tectiglobus diatomicola'–*Haslea* symbioses. a–**d**, Confocal laser scanning microscopy images (**a**,**b**) and corresponding scanning electron micrographs (**c**,**d**) of dividing diatoms with six (**a**,**c**) and eight (**b**,**d**) '*Ca*. T. diatomicola' cells, after hybridization with oligonucleotide probes (in pink, overlay of Hypho1147 and Hypho734 in red and blue, respectively; see Extended Data Table 2) and counterstaining with DAPI (white). Solid and dashed lines indicate assumed outline of the dividing diatoms. **e**, Confocal laser scanning microscopy image of a *Haslea* diatom after CARD-FISH with the NON338-probe showing no unspecific binding at the typical symbiont location (autofluorescence of the chloroplasts at 488 nm in green, NON338-probe background signal in light blue, DAPI in white). **f**, Epifluorescence image of the '*Ca*. T. diatomicola'–*Haslea* symbiosis, showing '*Ca*. T. diatomicola' cells after hybridization with a specific oligonucleotide probe (Hypho638 in blue), autofluorescence of the chloroplasts in green and the H-shaped nucleus counterstained with DAPI (white). The bilobed chloroplasts are located on either side of the central valve area, and the lobes of the chloroplasts are connected along the cell's transapical axis. **g**–**k**, Scanning electron micrographs of the diatom host. **g**, Whole frustule showing the internal raphe structure and an apparent hyaline area around the central raphe region (arrow) as well as sections of the hyaline girdle bands (arrowheads). **h**, Valve end showing the ridges bordering the central raphe. **i**, Central valve area. The valve's normal surface structure of longitudinal ribs overlying the transapical striae appears modified with the longitudinal ribs damaged and only the transapical structures visible. **j**, Valve pole showing the shape of raphe end (arrow head). **k**, Central valve area with the central valve area collapsed. Arrowheads point to a chamber-like structure. Scale bars are 5 µm in **a**–**g** and 1 µm in **h**–**k**.

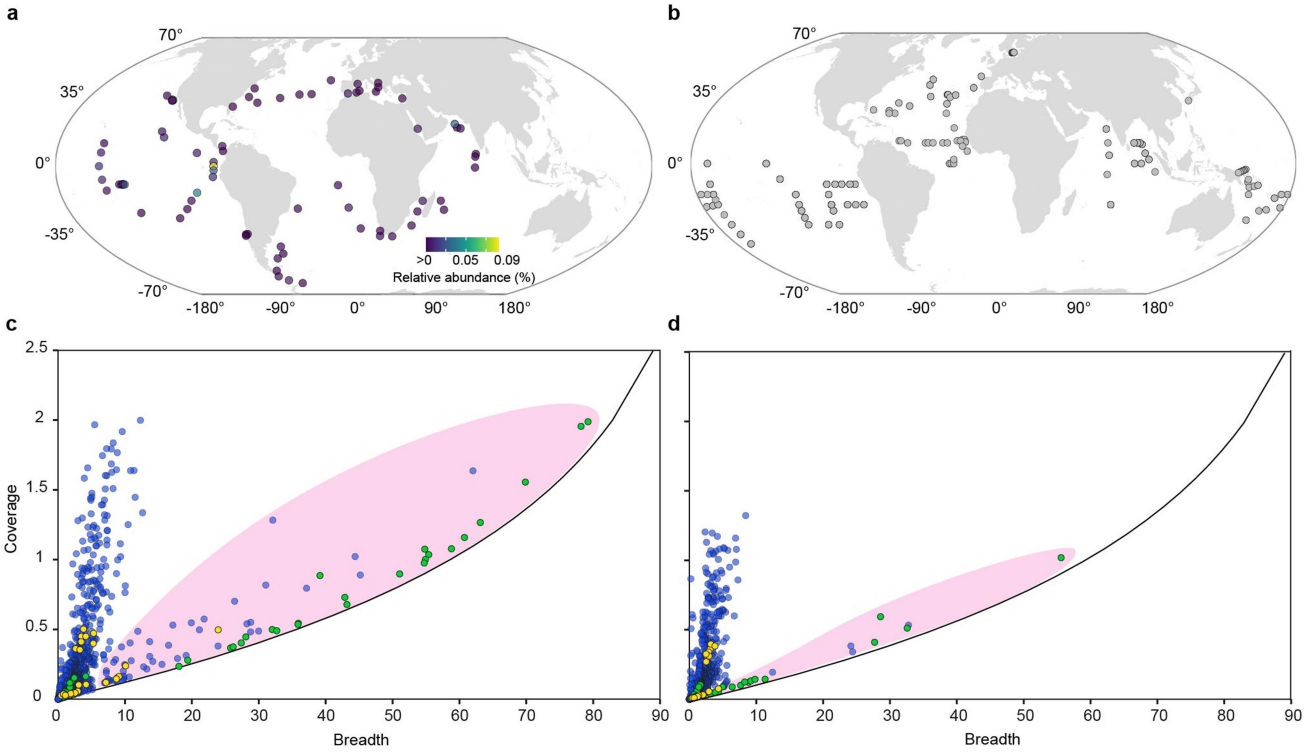

Extended Data Fig. 5 | Detection of '*Candidatus* Tectiglobus' and *Haslea* species in metagenomic and *nifH* qPCR datasets. a, Relative abundance of *Haslea* in the 0.8 to 5 µm size fraction determined from V9-18S rRNA amplicon sequencing data from Tara Oceans[96]. **b**, qPCR datasets in which no '*Ca*. T. diatomicola' *nifH* were detected (grey circles; data from Shao et al. [8,67]). **c**,**d**, Identification of '*Ca*. Tectiglobus' in metagenomes from Tara Oceans (blue), the South Pacific gyre (yellow) and the tropical North Atlantic (green) datasets. Coverage and breadth (fraction of the genome covered by at least one read) of the '*Ca*. T. diatomicola' (**c**) and '*Ca*. T. profundi' (**d**) genomes within the metagenomic samples. The black line indicates the expected breadth, see Methods. '*Ca*. Tectiglobus' was only considered to be present in metagenomes where the actual breadth was close to the expected breadth (all metagenomes inside the pink-shaded ellipses).

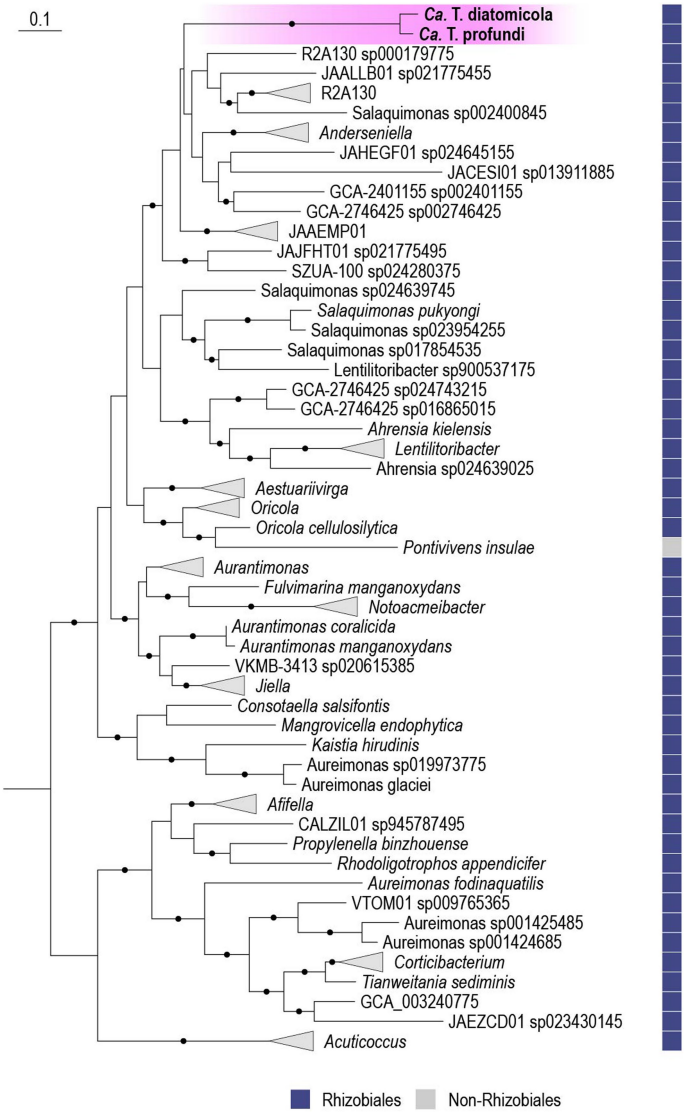

Extended Data Fig. 6 | Maximum likelihood phylogenetic tree of the '*Candidatus* Tectiglobus diatomicola' and '*Candidatus* Tectiglobus profundi' high-affinity cytochrome cbb_3-type terminal oxidase. The tree is constructed from closely related full-length CcoN amino acid sequences retrieved from the GTDB. The CcoN sequences of the two '*Ca*. Tectiglobus' species are highlighted in pink. The coloured squares indicate the taxonomic affiliation of the genome. Black dots indicate > 95% bootstrap support. Scale bar indicates amino acid substitutions per site.

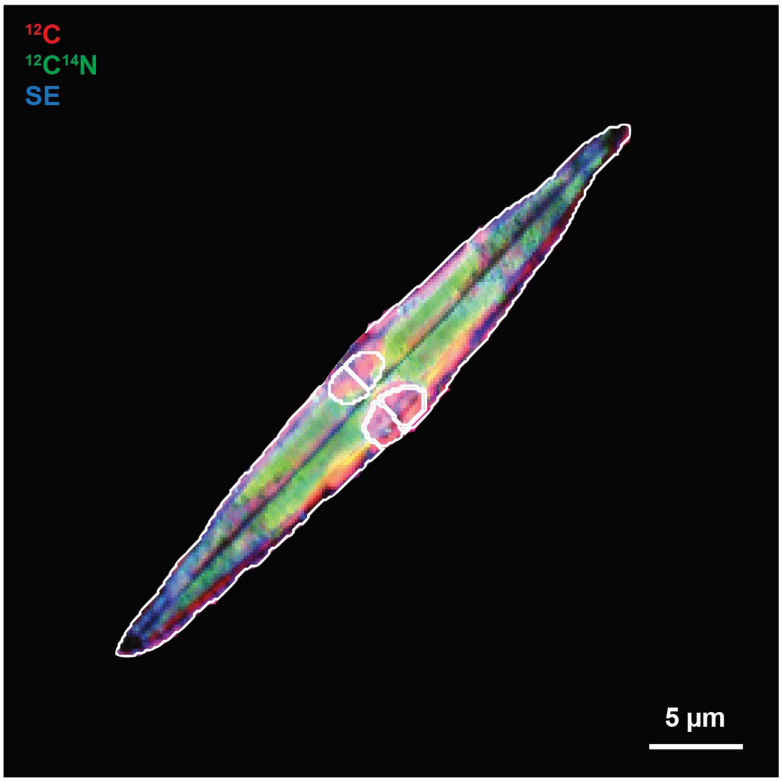

Extended Data Fig. 7 | Single-cell elemental imaging of the '*Candidatus* Tectiglobus diatomicola'–*Haslea* symbiosis. NanoSIMS image of the distribution of carbon (^{12}C, red) and nitrogen ($^{12}C^{14}N$, green) showing the carbon-rich symbionts embedded in nitrogen-rich host biomass. The image shows the same '*Ca*. T. diatomicola'–*Haslea* symbiosis as in Fig. 3a,b. SE, secondary electrons. Scale bar, 5 µm.

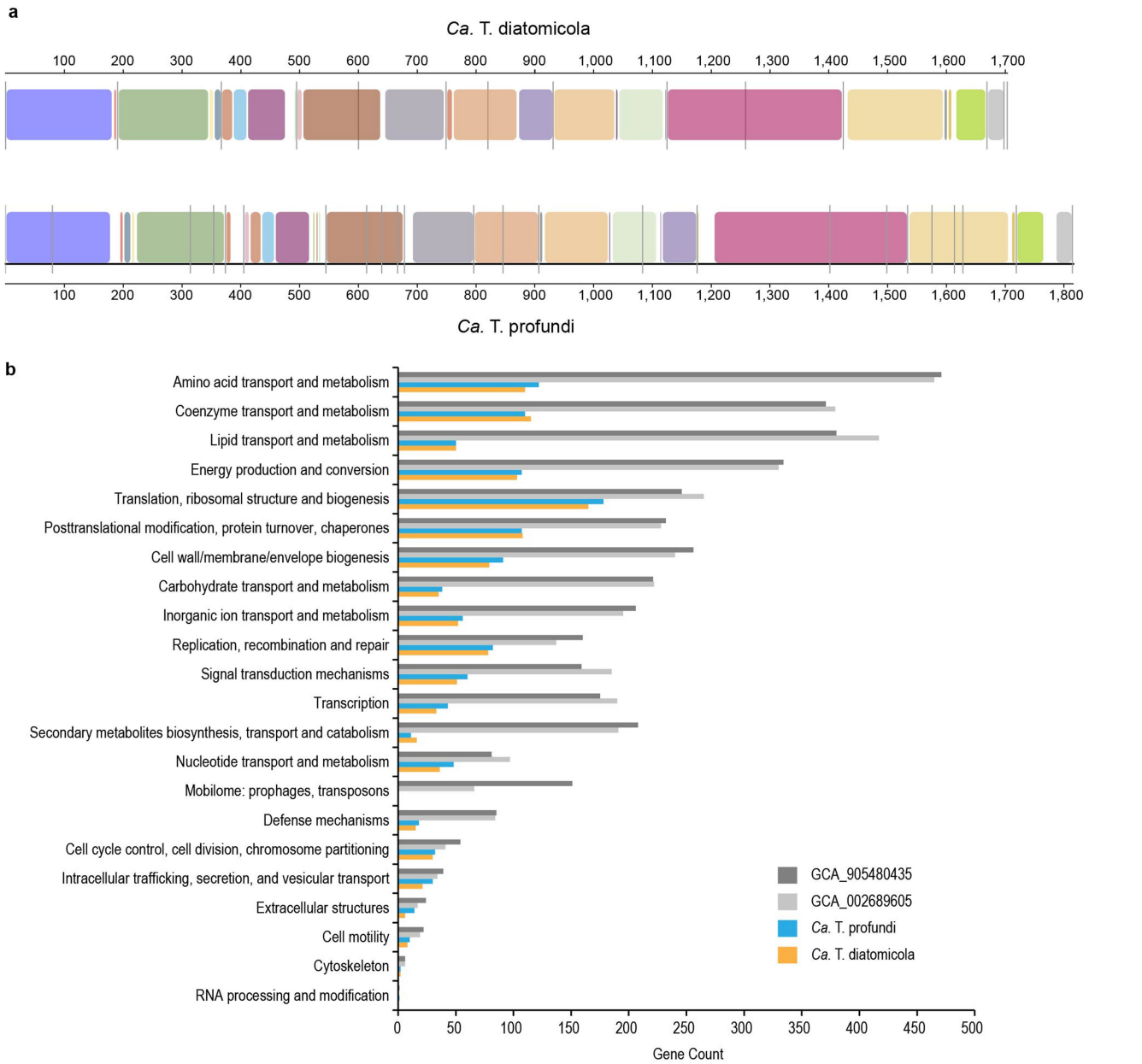

Extended Data Fig. 8 | Genome comparison of '*Candidatus* T. diatomicola' and '*Candidatus* T. profundi'. a, Whole-genome alignment of '*Ca*. T. diatomicola' (top) and '*Ca*. T. profundi' (bottom). Coloured boxes represent colinear regions present in both genomes. Grey vertical lines indicate contig boundaries. Numbers represent genomic positions in kilobase. **b**, Distribution of genes among the COG functional gene categories for the genomes of '*Ca*. T. diatomicola', '*Ca*. T. profundi' and their two closest relatives (GCA_905480435 and GCA_002689605).

Extended Data Table 1 | Abundances and single-cell activities of diatom symbioses in the tropical North Atlantic

Station	Total N_2 fixation (nmol N L^{-1} d^{-1})	Symbiosis	C-based growth rate (d^{-1})	Abundance (10^3 L^{-1})	N_2 fixation per symbiosis (fmol N $symb.^{-1}$ d^{-1})	Contribution of symbioses (nmol N L^{-1} d^{-1})
MSM89 S1 13.8°N 57.2°W	3.4 ± 0.4	*Ca.* T.diatomicola - *Haslea*	0.9 (4)	3.5	674 (4)	2.37
		Richelia-Guinardia		n.d.	-	-
		Richelia-Hemiaulus	0.4 (4)	0.09	4473 (4)	0.39
MSM89 S4 11.8°N 57.3°W	38.6 ± 6.8	*Ca.* T.diatomicola - *Haslea*	0.6 (4)	2.3	524 (4)	1.22
		Richelia-Guinardia		0.13	24209†	3.03
		Richelia-Hemiaulus		0.02	5450‡	0.08
MSM89 S13 10.8°N 57.8°W	31.0 ± 4.3	*Ca.* T.diatomicola - *Haslea*	0.8 (8)	2.3	739 (8)	1.71
		Richelia-Guinardia	0.8 (2)	0.05	61989 (2)	2.91
		Richelia-Hemiaulus		0.06	5450‡	0.34
M161 S4 12.1°N 57.2°W	25.3 ± 1.8	*Ca.* T.diatomicola- *Haslea*		1.2	646*	0.78
		Richelia-Guinardia	0.1 (5)	0.07	5925 (5)	0.41
		Richelia-Hemiaulus		n.d.	-	-
M161 S7 12.6°N 57.6°W	10.9 ± 2.0	*Ca.* T.diatomicola- *Haslea*		2.1	646*	1.34
		Richelia-Guinardia	0.1 (9)	0.1	4714 (9)	0.46
		Richelia-Hemiaulus	0.1 (2)	0.04	6427 (2)	0.23

*Calculated based on rate measurements at stations 1, 4 and 13 of MSM89 cruise.
† Calculated based on rate measurements at station 13 of MSM89 cruise and stations 4 and 7 of M161 cruise.
‡ Calculated based on mean of the rate measurements of station 1 of MSM89 cruise and station 7 of M161 cruise.

N_2 fixation rates and abundances of '*Ca.* T. diatomicola'–*Haslea*, *Richelia*–*Guinardia* and *Richelia*–*Hemiaulus* symbioses and their contribution to the total N_2 fixation rates at five different stations in the tropical North Atlantic. n.d. not detected. The number of diatom symbioses measured on nanoSIMS is shown in parentheses.

Extended Data Table 2 | Summary of 16S-rRNA-targeted oligonucleotide probes used for FISH

Probe	Target Organism	Probe sequence (5' to 3')	%FA
Hypho638	*Ca*. T. diatomicola	CTCTCTCGGACTCAAGACTAGCAGTATTG	45
used with	Competitor638	CTCTCTCGAACTCAAGACTAGCAGTATTA	45
Hypho825	*Ca*. T. diatomicola	CCGAAAAGCAAGCTTTCCAACAGCTAGC	45
used with	Helper854	GCTTAATGCGTTAGCTGCGCCA	45
Hypho1147	Many *Hyphomicrobiaceae*	GCTTATCACCGGCAGTCCCACTAG	40
used with	Helper1116 (specific to *Ca*. T. diatomicola)	GCCCAACTGAATGATGGCAACTAGCAGCG	40
Hypho734	several members of the genera *Filomicrobium*, *Hyphomicrobium* and *Pedomicobium*	CGTCAGTACCGATCCAGTGAGC	30
used with	Helper655	CACTCACCTCTCTCGGACT	30

Probe names are listed with their target organisms, sequences and percentage of formamide (%FA) used during hybridization.

nature portfolio

Corresponding author(s): Marcel Kuypers

Last updated by author(s): Apr 17, 2024

Reporting Summary

Nature Portfolio wishes to improve the reproducibility of the work that we publish. This form provides structure for consistency and transparency in reporting. For further information on Nature Portfolio policies, see our Editorial Policies and the Editorial Policy Checklist.

Statistics

For all statistical analyses, confirm that the following items are present in the figure legend, table legend, main text, or Methods section.

n/a	Confirmed	
☐	☒	The exact sample size (*n*) for each experimental group/condition, given as a discrete number and unit of measurement
☐	☒	A statement on whether measurements were taken from distinct samples or whether the same sample was measured repeatedly
☒	☐	The statistical test(s) used AND whether they are one- or two-sided *Only common tests should be described solely by name; describe more complex techniques in the Methods section.*
☒	☐	A description of all covariates tested
☒	☐	A description of any assumptions or corrections, such as tests of normality and adjustment for multiple comparisons
☐	☒	A full description of the statistical parameters including central tendency (e.g. means) or other basic estimates (e.g. regression coefficient) AND variation (e.g. standard deviation) or associated estimates of uncertainty (e.g. confidence intervals)
☒	☐	For null hypothesis testing, the test statistic (e.g. *F*, *t*, *r*) with confidence intervals, effect sizes, degrees of freedom and *P* value noted *Give P values as exact values whenever suitable.*
☒	☐	For Bayesian analysis, information on the choice of priors and Markov chain Monte Carlo settings
☒	☐	For hierarchical and complex designs, identification of the appropriate level for tests and full reporting of outcomes
☒	☐	Estimates of effect sizes (e.g. Cohen's *d*, Pearson's *r*), indicating how they were calculated

Our web collection on statistics for biologists contains articles on many of the points above.

Software and code

Policy information about availability of computer code

Data collection	Zeiss ZEN 3.2 blue edition; for the acquisition of raw mass spectrometric data, instrument-supplied software was utilized; also see Methods and Supplementary Information.
Data analysis	Trimmomatic v0.39, MEGAHIT v1.2.9, anvi'o v7.1 and v8, BLAST+ v2.9.0, minimap2 v2.22-r1101, SAMtools v1.14, CoverM v0.6.1, seqkit v2.3.0, SPAdes v3.15.3, CheckM2 v0.1.2, GTDB-TK v2.1.0, Prokka v1.14.6, DIAMOND v2.0.8, SqueezeMeta v1.6.2, mauve development snapshot 2015-02-26, muscle v3.8.1551, IQ-TREE v2.2.0.3 and v2.2.2.7, iToL v6.8.1, BWA-MEM v0.7.17-r1188, featureCounts v2.0.1, BRIG v0.95, DNAPlotter v18.1.0, bbmap v38.70/v38.87/v38.98, R v4.0.2, hifiasm-meta v0.2-r043, CompareM v0.1.2, fastANI v1.33, USEARCH v11.0.667, FastTree v2.1.11, MAFFT v7.505, trimAl v1.4.1, Barrnap 0.9-dev, HMMER v3.1b2 and v3.3.2, prodigal v2.6.3, Bowtie2 v2.3.4.1, MetaBAT 2 v2.12.1, MaxBin 2.0, CONCOCT v1.1.0, DAS Tool v1.1.1, ARB version arb-devel-7.1.rev19270, daime v2.2.2, Look@nanoSIMS v2018, UFBoot2, ModelFinder, RDP classifier v2.10.2, web servers: RAST, NCBI BLAST, MathFISH (no version numbers available), InterPro v95.0-98.0. Custom scripts for iterative bin refinements are deposited at https://github.com/bresyd/mag_refinement/tree/main

For manuscripts utilizing custom algorithms or software that are central to the research but not yet described in published literature, software must be made available to editors and reviewers. We strongly encourage code deposition in a community repository (e.g. GitHub). See the Nature Portfolio guidelines for submitting code & software for further information.

Data

Policy information about availability of data

All manuscripts must include a data availability statement. This statement should provide the following information, where applicable:

- Accession codes, unique identifiers, or web links for publicly available datasets
- A description of any restrictions on data availability
- For clinical datasets or third party data, please ensure that the statement adheres to our policy

Read data from metagenomic analyses pertaining to Ca. T. diatomicola have been deposited at the NCBI under BioProject accession number PRJNA1036431, including the MAGs of Ca. T. diatomicola and Ca. T. profundi under the accession numbers JAZDSJ000000000 and DAWWJP000000000, respectively. RNA sequencing data can be found under the same bioproject number with the accession numbers SRR26695118, SRR26695119 and SRR26695121- SRR26695130. The publicly available sequences used for phylogenetic tree construction and genome comparison can be found at the Genome Taxonomy Database (GTDB; https://gtdb.ecogenomic.org/) under the accession numbers given in Supplementary Data 1-9 (tree file for each tree). Publicly available MAGs from Delmont et al. (2022) can be found under https://figshare.com/articles/dataset/Marine_diazotrophs/14248283. Tara ocean metagenomes used in this study can be found under https://www.ncbi.nlm.nih.gov/bioproject/173486 with the following bioprojects used in this study: PRJEB4352 (size fractions for protists; https://www.ncbi.nlm.nih.gov/bioproject/213098), PRJEB1787 (size fractions for prokaryotes; https://www.ncbi.nlm.nih.gov/bioproject/196960), PRJEB9691 (size fractions for protists from polar circle samples; https://www.ncbi.nlm.nih.gov/bioproject/287904), PRJEB9740 (size fractions for prokaryotes from polar circle samples; https://www.ncbi.nlm.nih.gov/bioproject/288558).
For the reconstruction of the MAG of Ca. T. profundi, the used metagenomic data can be found at the GTDB under: https://gtdb.ecogenomic.org/genome?gid=GCA_013214245.1 (original MAG) as well as the Sequence Read Archive under: https://www.ncbi.nlm.nih.gov/bioproject/PRJNA482655 with the accession numbers SRR7648332, SRR7648341, SRR7648350, SRR7632647, SRR7648334 (metagenomes used for MAG reconstruction). Publicly available qPCR data from Shao et al. (2023) can be found under: https://doi.org/10.6084/m9.figshare.21677687.v3. Additional databases used in this study can found under the following links: eggNOG: http://eggnog45.embl.de/download/eggnog_4.5/data/NOG/, ncbi-nr database: https://ftp.ncbi.nlm.nih.gov/blast/db/FASTA/nr.gz, pfam database: https://www.ebi.ac.uk/interpro/download/pfam/, kegg database: http://andes.cnb.csic.es/SqueezeMeta/kegg.db.gz. Source data are provided with this paper.

Research involving human participants, their data, or biological material

Policy information about studies with human participants or human data. See also policy information about sex, gender (identity/presentation), and sexual orientation and race, ethnicity and racism.

Reporting on sex and gender	N/A
Reporting on race, ethnicity, or other socially relevant groupings	N/A
Population characteristics	N/A
Recruitment	N/A
Ethics oversight	N/A

Note that full information on the approval of the study protocol must also be provided in the manuscript.

Field-specific reporting

Please select the one below that is the best fit for your research. If you are not sure, read the appropriate sections before making your selection.

☐ Life sciences ☐ Behavioural & social sciences ☒ Ecological, evolutionary & environmental sciences

For a reference copy of the document with all sections, see nature.com/documents/nr-reporting-summary-flat.pdf

Ecological, evolutionary & environmental sciences study design

All studies must disclose on these points even when the disclosure is negative.

Study description	The study is based on two parallel cruises (R/V MARIA S. MERIAN (cruise MSM89; Bridgetown, Barbados – Bridgetown, Barbados) and R/V METEOR (cruise M161; Bridgetown, Barbados – Ponta Delgada, Azores, Portugal) in January/February 2020 in the western tropical North Atlantic. The aim of our participation on these cruises was to determine nitrogen fixation rates and identify N2 fixers present in this region. For this, on-deck experiments were carried out to determine in-situ N and C fixation rates in surface water samples (with incubations going for 24 hrs from dawn to dawn). At the same time, microbial biomass from surface waters was sampled using filtration for subsequent DNA/RNA extractions and sequencing, to identify potential novel N2-fixers and study their metabolic potential. Samples were also for visualization of specific microorganims using FISH and determination of single cell rates using nanoSIMS.
Research sample	The tropical North Atlantic is an area known to harbor an active community of N2-fixers (accounting for ~20% of the oceanic N2

Research sample	fixation). It was also known that typical N2 fixers can not account for the bulk rates previously measured in this area. The combination of high N2 fixation and the potential presence of so far unknown N2-fixers was the crucial factor for our decision to chose this study site. In detail, we report results from sequencing data and/or incubation experiments from eight different surface water stations (six from the MSM89 and two from the M161 cruise).
Sampling strategy	No statistical methods were used to pre-determine sample size. Sampling size was largely determined by the feasibility of experiments with incubation experiments carried out in triplicates for each station. Please also refer to the methods section.
Data collection	Surface water for all experiments and samples was collected using rosette samplers equipped with CTD (conductivity-temperature-depth) systems and Niskin bottles by the CTD team on each cruise. Biomass and mass spectrometric data was collected using an elemental analyzer coupled to a continuous-flow isotope ratio mass spectrometer (equipped with an autosampler, operated by technical support staff), a nanoscale secondary ion mass spectrometer (operated by Abiel Kidane and technical support staff), a gas chromatograph and a gas chromatograph coupled to an isotope ratio mass spectrometer (operated by technical support staff). Sequencing data was generated at the Max Planck Genome Centre Cologne (individual sequencing platforms are detailed in the methods section).
Timing and spatial scale	The two parallel cruises took place during January/February 2020. This study reports data from a total of eight stations within an area from 13.7720 - 10.769 °N and 57.7815 - 57.2454 °W that were visited during that time frame.
Data exclusions	No data were excluded from analyses.
Reproducibility	All experiments described in our study come from come from two parallel cruises visiting distinct locations at different days. Within each set of experiments, triplicate incubations and multiple measurements within each triplicate (where applicable) were performed to assess variability. Variability within triplicates was substantial (see Extended Data Table 1) reflecting biological differences between individual microbial communities and in-situ conditions rather than errors in measurements. All attempts at replication were successful.
Randomization	The location for sampling was selected randomly depending on the position of the vessels at dawn on the days of the stations.
Blinding	Blinding was not pertinent to our study because it did not include any animals and/or human research participants. In addition, blinding was not possible since many analyses were also carried out by the persons in charge of sampling and interpretation of the data was done by persons in charge of analyses.

Did the study involve field work? ☒ Yes ☐ No

Field work, collection and transport

Field conditions	Overall, the weather conditions during the two parallel cruises were calm with only some intermittent light rain. The surface water temperature at the stations was ~27 °C.
Location	The dates and locations of the eight stations are as follows: MSM89-S1 (1/19/2020; 13.7720 °N 57.2483 °W), MSM89-S2 (1/21/2020; 12.7599 °N 57.6089 °W), MSM89-S4 (1/25/2020; 11.8008 °N 57.2755 °W), MSM89-S10 (2/7/2020; 12.4191 °N 57.2454 °W), MSM89-S13 (2/14/2020; 10.769 °N 57.7815 °W), MSM89-S14 (2/16/2020; 11.0519 °N 57.2798 °W), M161-S4 (1/27/2020; 12.125 °N 57.2456 °W), M161-S7 (2/4/2020; 12.5879 °N 57.6069 °W).
Access & import/export	Samples were collected and exported in compliance with local, national and international regulations. Permissions to conduct marine scientific research in territorial waters were issued by the Ministry of Foreign Affairs and Foreign Trade in Barbados (No. IR/2020/08 and IR/2020/09; issued January 15th, 2020) and the Ministry of Foreign and CARICOM Affairs of the Republic of Trinidad and Tobago (No. 2053; issued November 12th, 2019).
Disturbance	No disturbances were caused by this study.

Reporting for specific materials, systems and methods

We require information from authors about some types of materials, experimental systems and methods used in many studies. Here, indicate whether each material, system or method listed is relevant to your study. If you are not sure if a list item applies to your research, read the appropriate section before selecting a response.

Materials & experimental systems

n/a	Involved in the study
☒	☐ Antibodies
☒	☐ Eukaryotic cell lines
☒	☐ Palaeontology and archaeology
☒	☐ Animals and other organisms
☒	☐ Clinical data
☒	☐ Dual use research of concern
☒	☐ Plants

Methods

n/a	Involved in the study
☒	☐ ChIP-seq
☒	☐ Flow cytometry
☒	☐ MRI-based neuroimaging

Plants

Seed stocks	N/A
Novel plant genotypes	N/A
Authentication	NA